5-2017

On-Line Estimation of Oxygen Transfer Rate with Oxygen Enriched Air using Off-Gas Sensor for Escherichia coli

Mohammad Mayyan
Clemson University, mhmayyan@gmail.com

On-Line Estimation of Oxygen Transfer Rate with Oxygen Enriched Air using Off-Gas Sensor for Escherichia coli

---

A Thesis
Presented to
the Graduate School of
Clemson University

In Partial Fulfillment
of the Requirements for the Degree
Master of Science
Electrical Engineering

---

by
Mohammad Mayyan
May 2017

Accepted by:
Dr. Richard Groff, Committee Chair
Dr. Sarah Harcum
Dr. Adam Hoover

Abstract

An online estimator for the Oxygen Transfer Rate OTR for *Escherichia coli* cultured in bioreactors was developed, which allowed for improved culture outcomes. *E.coli* are used to manufacture recombinant proteins used as therapeutics, such as insulin and human growth hormone. *E.coli* cultures require high levels of oxygen in order to produce the therapeutics efficiently. Previous methods to estimate OTR used values for the volumetric mass transfer coefficient, k_La, which had been determined from separate experiments and thus set to a constant value or by stopping oxygen flow periodically to the bioreactor to update the k_La value. In this work, the k_La value was estimated in real-time and continuously from the on-line dissolved oxygen concentration and off-gas measurements. The gas phase mixing in the head space and time response of the off-gas sensor were accounted for in the model. The improved estimates of OTR were incorporated into a model of *E.coli* metabolism to better predict the metabolic state of *E.coli*, such that glucose could be fed to *E.coli* at near optimal rates. Additionally, the effects of enriching the air with pure oxygen were accounted for in the estimator model, as this enrichment is necessary to reach final cell densities representative of the industrial process.

Dedication

I dedicate this work to my parents, wife, and beautiful children.

Acknowledgments

First and at most, I would like to thank my research and academic advisor Dr. Richard Groff, for the support and directions to overcome all the problems and challenges I found during the research until the end of writing this thesis. I would also like to thank Dr. Sarah Harcum for the guidance and help she gave me during the research, and to thank Dr. Adam Hoover for teaching me all the valuable knowledge and skills which have helped me a lot in my research and in my life.

I would also like to express my thanks to my research fellows Mr. Shahin Lashkari, and Dr. Matthew Pepper, and to thank Ms. Aswini Vijayaraghavan and Mr. Tom Caldwell.

Table of Contents

List of Tables

List of Figures

Chapter 1

Introduction

In the biopharmaceutical industry, simple proteins are produced using bacterial cultures, where recombinant *Escherichia coli*(*E.coli*) is the most common. The types of biopharmaceutical made in *E.coli* include insulin, human growth hormone (hGH), and some anticancer drugs [Sanchez-Garcia et al., 2016].

In order to culture *E.coli* in large quantities, cost effective computer controlled bioreactors, which are set to control temperature, pH, and Dissolved Oxygen (DO), and to feed the culture over time to assure biomass growth and hence more protein production. Many different control methods have been used to maximize the protein production by controlling the feed rate. One of these control methods uses the Oxygen Uptake Rate (OUR) to determine the feed rate. This work developed an improved estimator for OUR for *E.coli* cultures cultivated in a bioreactor.

1.1 Bioreactors

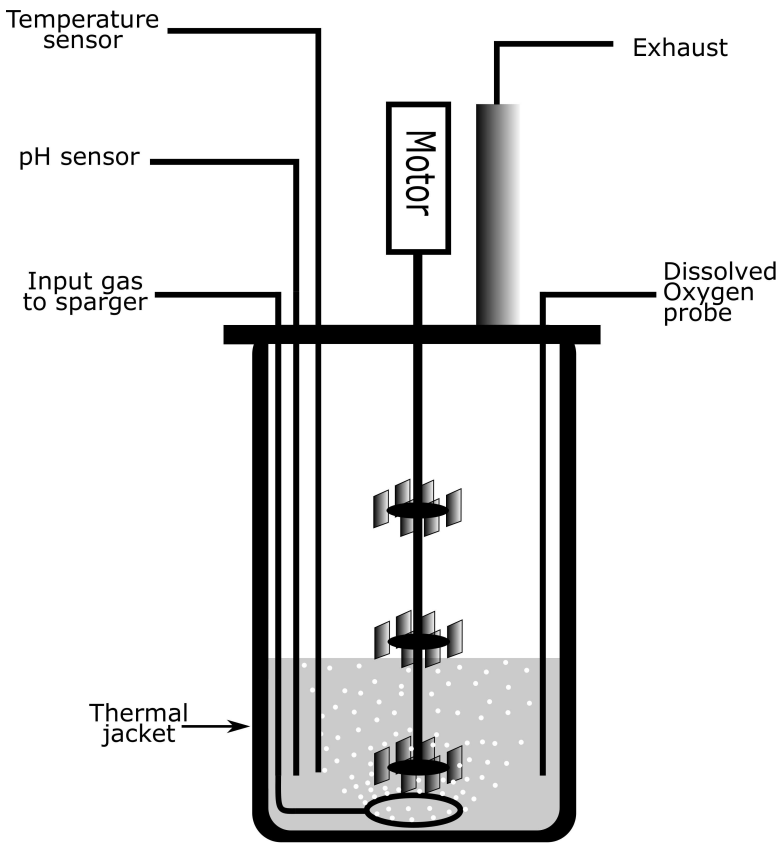

Figure 1.1: Basic bioreactor system.

Industrial fermenters, or bioreactors, are used to cultivate suspensions of cells. A bioreactor is a vessel that provides required conditions for a biochemical process. Figure 1.1 shows a typical configuration of a bioreactor. Aeration tube ending with a sparger provides any needed input gas or a mixture of gases; i.e., O_2, Air, or CO_2. Impeller blades are connected via a shaft to an agitator to stir the culture medium and break down the sparge gas into smaller bubbles for a higher surface contact between the bubbles and the culture medium so that the sparge gas dissolves in the medium at a higher rate. The spinning blades cause the medium to rotate in a centrifugal pattern towards the wall of the vessel, where baffles, located at the vessel wall, are used to form obstacles and push the medium back to the spinning blades for an effective mixing.

A metal head plate with a polymeric O-ring is used to seal the vessel and most of the control instruments are connected via this plate. Temperature, dissolved oxygen, and pH probes

are connected as input signals to a digital control unit (DCU) to regulate the fermentation process and provide the required conditioning for the cells to grow. A water jacket (heat exchanger system), agitator, and a pump are controlled by the DCU to keep the culture temperature, dissolved oxygen, and pH, respectively, at desired levels. Pumps can also be used to control nutrient additions. After the start of the fermentation, nutrients are added. This process is called fed-batch. The fed-batch phase usually starts at the end of a batch phase in which the culture grows using the initial amount of the nutrient.

A continuous flow of filtered air is used to provide the culture with oxygen. The amount of oxygen in air is, usually, insufficient for high cell density to remain aerobic. Air is normally mixed with oxygen to increase the oxygen mole ratio in the sparge gas. This technique is used to increase the dissolved oxygen when the agitator speed approaches the maximum rotation speed. Thus, gas mixing enables the culture to grow to higher cell densities.

1.2 Purpose of Metabolism Controlling

Usually, the process of cultivation starts with a sterile culture medium inside the bioreactor, which is set up in a batch operation with some amount of initial substrate (nutrient). The culture is then inoculated with some amount of cells. During the cultivation process, the culture is kept at the desired temperature. Base is added to keep the culture at a desired pH levels. A continuous flow of air is maintained to provide sufficient dissolved oxygen required for oxidative metabolism. At the end of the batch phase, fed-batch starts to prevent substrate depletion and to keep cells growth rate at a high level. When substrate concentration exceeds a certain level, growth rate increases and cells start entering overflow metabolic state in which the substrate consumption occurs without the involvement of oxygen in the chemical process. *E.coli* produces acetate during overflow metabolism.

When biomass reaches a specified cell density, the culture is induced by a chemical agent to start recombinant protein production. It is desired to maximize the protein production and minimize the production of acetate that inhibits growth [Luli and Strohl, 1990] and reduces protein production [Jensen and Carlsen, 1990]. To achieve this goal, the feed rates have been experimentally determined to keep growth rate high enough while low enough to prevent acetate production. Under this control strategy, the recombinant protein production is maximized. This control strategy could be achieved withou human interaction by monitoring the OUR as suggested by [Pepper, 2015], which requires

an on-line monitoring of OUR signal.

A real-time adaptive estimator of the Oxygen Transfer Rate (OTR) using an off-gas sensor was implemented by [Wang, 2014], and was used by [Pepper, 2015] in his control algorithm. The OTR was estimated from dissolved oxygen measurements and a volumetric mass transfer coefficient k_La, which was continuously updated using off-gas measurements. The OTR estimator was limited to working with air as the input gas, thus could not be used to culture *E.coli* to high-cell densities, where oxygen enriched air was required. The focus of the current work was to extend the OTR estimator to function with variable oxygen enriched air as the input sparge gas, and to demonstrate that *E.coli* could be cultured to high-cell densities and adapting the feed rate.

1.3 Prior Work

This section is divided into two subsections. First, an overview is presented for computing the oxygen transfer rate OTR and the need for having a real-time estimate for the volumetric transfer rate coefficient k_La. Second, methods used to increase the oxygen transfer rate are discussed.

1.3.1 Computing the OTR

Aerobic biological processes need sufficient dissolved oxygen to function, thus accurate calculation or estimation of OTR is very important for process scale-up or prediction of metabolic states. The key to OTR calculation is the accurate estimate of the volumetric transfer rate coefficient k_La. Several different methods are used to estimate k_La. Theses methods can be classified into two main groups: based on the presence or absence of biological consumption of oxygen [Garcia-Ochoa and Gomez, 2009]. The problem of finding k_La without biological consumption of oxygen is that once the medium is inoculated with the microorganisms, k_La will change due to the oxygen consumption itself [Vashitz et al., 1989] and due to the change in the medium composition and its physical properties by secretion of waste products by the microorganism. Therefore, for this work, OTR estimates were only considered in the presence of the biological consumption of oxygen.

In presence of microorganisms, dynamic methods are most commonly used to estimate k_La . The most common method turns off the inflow gas supply, OUR is obtained by the slope of decreasing dissolved oxygen concentration. The gas supply is turned on and the dissolved oxygen concentration increases back to steady state. Using the time profile, k_La is computed [Bandyopadhyay et al., 1967].

This method has several limitations such as the time response of the dissolved oxygen probe should be accounted for. In addition, the dissolved oxygen concentration required for the microorganisms should not decrease below a critical level to prevent periods of non-optimal growth. Modifications of this method have been proposed to overcome these limitations. The time response of the dissolved oxygen probe was accounted for to more accurately estimate the k_La [Badino et al., 2000]. Another change to the dynamic method was to use oxygen enriched air instead of stopping the flow of air in order to change the dissolved oxygen concentration and thus estimate k_La and to also account fro the time response of the dissolved oxygen probe [Kim and Chang, 1989]. k_La was also estimated by applying series of changes in the stir speed and/or in gas flow rate, and the time response of the dissolved oxygen probe was also accounted for [Patel and Thibault, 2009].

k_La can also be estimated using gas analyzers in the inflow and outflow in presence of biological consumption of oxygen. By measurements of oxygen mole ratios in the input and output gases of a bioreactor along with measurements of dissolved oxygen concentration in the culture liquid, k_La can be estimated under steady state conditions [Redmon et al., 1983]. Dilution effect of the off-gases, however, should be taken into consideration for the correct calculation of the OTR [Van't Riet, 1979]. This method has become simple and practical for bioreactors after the recent advances in off-gas sensors technology, i.e., using BlueSens single gas sensor for O2 and CO2 [BlueSens, nd]. This method needs two sensors, however, it enables for real time estimation for the k_La without the need for perturbing the dissolved oxygen concentration.

Other techniques using chemical reactions have also been proposed to find the k_La [Ortiz-Ochoa et al., 2005]. These techniques, however, might be time-consuming and the physical properties of the culture liquid could change due to the chemical additions. Physical techniques have also been proposed for the k_La determination, such as using radioactive materials [Pedersen et al., 1994], or dynamic pressure method [Carbajal and Tecante, 2004].

1.3.2 Increasing the OTR

The simplest way to increase the OTR is to use higher agitation speeds, which is limited by hardware specifications and some microbial strains die at high speeds of agitations. Therefore, cultivation of higher cell density is limited by OTR. To increase the OTR in bioreactors, there are mainly three techniques known in the literature: pressurizing the bioreactor, oxygen enrichment in input gas, and adding chemicals to the culture medium.

Some metal bioreactors can be pressurized to enhance the OTR. *E.coli* TB1 was used in fed-batch cultivations that require high levels of oxygen supply [Belo and Mota, 1998]. The study was to compare two cultivations having the same OTR, which was increased by two different ways. The first way was by increasing the stir speed while the pressure inside the bioreactor was kept around one [atm]. The second way was by pressurizing the bioreactor up to around 4.7 [atm] while the stir speed was kept low. A higher cell density and four-fold increase in the final productivity of the recombinant protein were achieved in the pressurized bioreactor compared with the lower pressure and higher stir speed. Higher oxygen supply was provided to the culture in the pressurized bioreactor.

Oxygen enrichment in the input gas is a very common technique for OTR enhancement. Compressed oxygen from a tank, for example, is mixed with another input gas, such as compressed air, using some instruments so that the mixed gas contains mole ratio of oxygen higher than that in the air. When 40% oxygen enriched air was used, for example, the produced biomass of *E.coli* was increased by 77% [Castan et al., 2002]. In a comparison between oxygen enriched air and pressurized bioreactor fed-batch cultivations, it was found that the OTR and the final biomass concentration were higher in the pressurized cultivation [Lara et al., 2011]. However, pressurizing the bioreactor cannot be implemented for many small-scale laboratory bioreactors.

OTR could also be enhanced chemically. An addition of perfluorocarbon emulsions to the culture medium, for example, has been studied to improve oxygen supply in a bioreactor for *E.coli* cultivation [Ju et al., 1991]. The result of the study demonstrated an enhancement in the oxygen transfer.

1.4 Thesis Statement

The aim of this work was to augment the adaptive OTR estimator for *E.coli* cultivation developed by [Wang, 2014] to have the capability to handle sparge gases with variable oxygen enrichment. The OTR adaptive estimator was modified to account the variable oxygen mole ratio in the input gas. In addition, a more accurate method was used to calculate the oxygen mole ratio in the input gas. The dissolved oxygen concentration was controlled by a PID controller. A variable gain that decreases over time was used for the OTR adaptive estimator.

1.5 Thesis Outline

The thesis is organized as follows, in Chapter 2, system configuration required to achieve the proposed solution will be presented along with the mathematical modifications used in OTR estimation. In addition, other design considerations will also be discussed. Results are presented and discussed in Chapter 3. Conclusions and future work will be presented in Chapter 4. Finally, the appendix will include other related work and more details about used algorithms, and settings and conditioning of all experiments used in this thesis.

Chapter 2

Research Design and Methods

Previous work developed method to estimate OTR in real-time from off-gas and dissolved oxygen concentration sensors. However, the inlet gas was limited to air. In this work, the OTR estimator was augmented to be capable of addressing enriched sparge gases. In this chapter, other design considerations for the OTR adaptive estimator are discussed. These considerations include the calculation of oxygen mole ratio in sparge gas, excitation of the input signal and the estimator gain.

Figure 2.1 shows the system configuration and connections used in this design. The Digital Control Unit (**DCU**) of the bioreactor controls the desired mole ratio of oxygen in the sparge air using input signal called **GasMx**, which could be set by a connected computer. The input gases are compressed air and oxygen which are regulated by pressure regulators PR-air and PR-O_2, respectively. A Mass Flow Meter (**MFM**) and Rotameter are used for measuring and tuning the sparge air flow rate. Off-gas sensor is used to measure oxygen mole ratio at the exhaust. Dissolved Oxygen (**DO**) is measured by the in-liquid autoclavable probe. A motor is used to control the dissolved oxygen level in the liquid. There are three equally spaced impeller blades connected to the stirrer shaft.

Acronym	***Unit***	***Definition***
τ_h	s	Head space time constant.
τ_b	s	Off-gas sensor time constant.
b_{in}	$\frac{\text{mol}}{\text{mol}}$	Oxygen concentration in the sparge air.
b_{SL}	$\frac{\text{mol}}{\text{mol}}$	Oxygen concentration at surface level of the culture media.
b_h	$\frac{\text{mol}}{\text{mol}}$	Oxygen concentration in off-gas at the headspace of the vessel.
b_{out}	$\frac{\text{mol}}{\text{mol}}$	Oxygen concentration measured by the off-gas sensor.
b_{air}	$\frac{\text{mol}}{\text{mol}}$	The mole ratio of oxygen in air ≈ 0.2096.
OUR	$\frac{\text{mol}}{\text{L·h}}$	Oxygen uptake rate.
$\widehat{OUR}$	$\frac{\text{mol}}{\text{L·h}}$	Estimated OUR.
k_La	s^{-1}	Volumetric oxygen transfer coefficient.
$\widehat{k_La}$	s^{-1}	Estimated k_La.
OTR	$\frac{\text{mol}}{\text{L·h}}$	Oxygen transfer rate computed using dissolved oxygen measurements.
$\widehat{OTR}$	$\frac{\text{mol}}{\text{L·h}}$	Estimated OTR.
$OTR_{off-gas}$	$\frac{\text{mol}}{\text{L·h}}$	Oxygen transfer rate computed using off-gas sensor measurements.
$OUR_{off-gas}$	$\frac{\text{mol}}{\text{L·h}}$	OUR computed using off-gas sensor measurements.
M_f	$\frac{\text{L}}{\text{h}}$	Mass flow.
ρ^α	bar	Normal pressure = 1.0133.
V_c	L	Volume of liquid in the bioreactor.
V_h	L	Volume of headspace in the bioreactor.
R	$\frac{\text{bar·L}}{\text{K·mol}}$	Gas constant $= 8.314 \times 10^{-2}$.
T	K	Temperature = 273.15 .

Table 2.1: List of acronyms

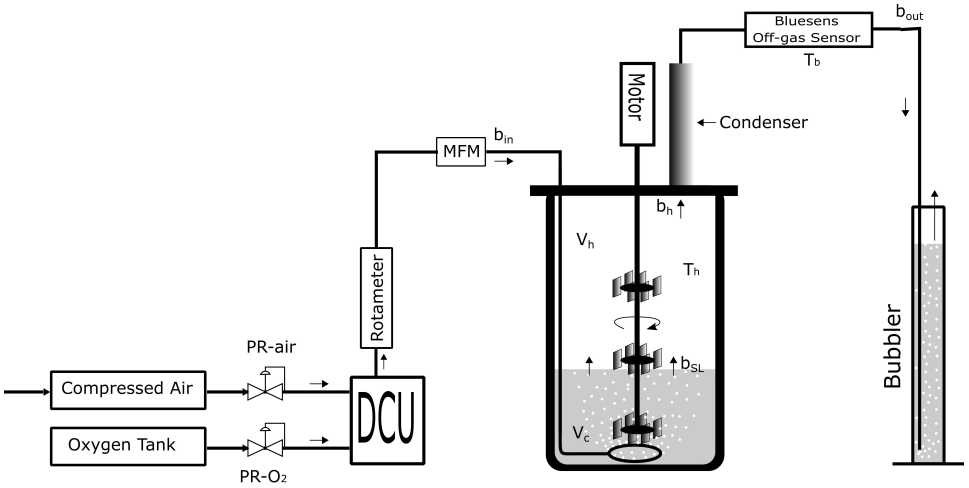

Figure 2.1: Bioreactor Connections.

2.1 OTR Calculations

Using measurements of oxygen and carbon dioxide mole ratios from off-gas sensor at the exhaust of the bioreactor, OTR can be calculated by

$$OTR_{off-gas} = \frac{M_f \cdot \rho_{O_2}}{V_c \cdot R \cdot T}(b_{in} - \frac{1 - b_{in} - d_{in}}{1 - b_{out} - d_{out}} \cdot b_{out}), \tag{2.1}$$

where the constants ρ_{O_2}, R, T, and d_{in}, are, respectively, the normal pressure [bar], ideal gas constant [$\mathrm{L \cdot bar \cdot K^{-1} \cdot mol^{-1}}$], culture temperature [K], and partial pressure of carbon dioxide in sparge air [BlueSens, nd]. Mass flow rate M_f [$\mathrm{L \cdot h^{-1}}$] was kept fixed for every experiment, but it could change from one experiment to another. Culture volume V_c [L] is used to normalize the OTR value, and it increased over time with feeding. Output oxygen b_{out} and carbon dioxide d_{out} concentrations at the exhaust are measured by the off-gas sensor. The oxygen concentration in the sparge air b_{in} was computed and will be explained in Section 2.5. For simplicity in mathematical expressions, the ratio

$$OG = \frac{1 - b_{in} - d_{in}}{1 - b_{out} - d_{out}} \tag{2.2}$$

refers to the ratio of other gases in the sparge air, excluding O_2 and CO_2, to other gases in the off gas and it is assumed to be one all the time ($OG = 1$) as shown in Figure 2.2. It was assumed that the culture does not consume nor does it produce gases other than oxygen and carbon dioxide, respectively. For calculation simplicity, Equation 2.1 could be rewritten as

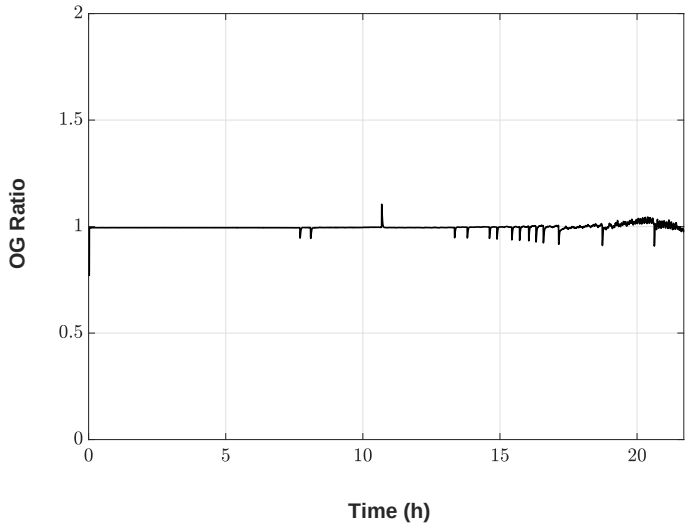

Figure 2.2: Plot of Equation 2.2.

$$OTR_{off-gas} = F_r(b_{in} - b_{out}) \tag{2.3}$$

which shows the oxygen demand, the difference between the oxygen concentrations in the sparge air and off-gas, multiplied by a scaling factor F_r.

$$F_r = \frac{M_f \cdot \rho_{O_2}}{V_c \cdot R \cdot T} \tag{2.4}$$

The OTR can also be calculated by

$$OTR = k_L a(C^* - C), \tag{2.5}$$

which is well known in the literature and it is a function of oxygen volumetric transfer coefficient $k_L a$ and a difference between the oxygen saturation concentration in the liquid phase C^* and the dissolved oxygen concentration C [Van Suijdam et al., 1978, Åkesson and Hagander, 1999]. The $k_L a$ coefficient is a function of many variable factors, such as agitator speed (N), gas flow rate (M_f), the solubility of the liquid, temperature, etc.

For simplifying the algorithm and implementation on computer, we refer to $(C^* - C)$ as the OTR driving force DF

$$DF = (C^* - C) \tag{2.6}$$

where C^* comes from Henry's law [Zumdahl, 2014], and it is the maximum concentration of oxygen that can dissolve in a liquid at P [atm] pressure and T [Kelvin] temperature. C^* could be calculated by

$$C^* = K \cdot \frac{b_{in}}{b_{air}} \tag{2.7}$$

where the ratio $\frac{b_{in}}{b_{air}}$ is used to scale C^* because of the oxygen enrichment in the sparge air and this one of the modifications to the OTR estimator developed by [Wang, 2014]. $b_{air} \approx 0.2096$ is the partial pressure of O_2 in air, and K is the solubility of oxygen that can dissolve in a liquid at P [atm] pressure and T [Kelvin] temperature. For our purpose, during the system setup, the dissolved oxygen probe is calibrated using: nitrogen to read zero and compressed air to read 100%. The measurement of dissolved oxygen probe at 100% corresponds to $K_0 = 2.1 \times 10^{-4}$ [$\text{mol} \cdot \text{L}^{-1}$], which is the maximum solubility of oxygen (contained in the compressed air b_{air}) in fresh water in equilibrium with one [atm] pressure at 37 [°C] temperature [Benson and Krause, 1980, Stewart A. Rounds and Ritz, 2013]. In our particular system, the pressure inside the bioreactor vessel is almost one atmospheric pressure all the time. Note that, K changes slowly over the course of the fermentation run due to the change in the liquid composition. At time zero, however, we use $K = K_0$. The dissolved oxygen concentration C is computed by

$$C = K_0 \cdot \frac{DO}{100} \tag{2.8}$$

where DO is the dissolved oxygen probe measurement. Equation 2.6 could be rewritten as

$$DF = (K \cdot \frac{b_{in}}{b_{air}} - K_0 \cdot \frac{DO}{100}) \tag{2.9}$$

For a fixed mass flow rate M_f, the k_La is commonly linearized using Taylor series expansion [Bastin and Dochain, 1990], and used as a function of the stir speed ($k_La \sim N$) as shown in the equation

$$k_La(N) = k_La(N_L) + \frac{dk_La}{dN}(N - N_L) = \alpha_0 + \alpha_1(N - N_L). \tag{2.10}$$

For simplicity, we use $N_L = 0$ and this is another modifications to the OTR estimator developed by [Wang, 2014]. k_La is, therefore, calculated by

$$k_La(N) = \alpha N \tag{2.11}$$

Equation 2.5 could be rewritten as

$$OTR = \alpha \cdot N \cdot DF. \tag{2.12}$$

Measurements of N and C, which are read from the control unit DCU within a sampling interval (15 seconds in our system), enable Equation 2.12 to give results faster than Equation 2.3, because the latter depends on off-gas measurement that is heavily filtered by the bioreactor headspace dilution time constant τ_h and the time constant of the off-gas sensor itself τ_b. The response time $t_{98}\%$ of the DO probe, however, is 30 to 60 seconds at 25 ℃, from air to nitrogen (given by the manufacturer, Hamilton OxyFerm FDA VP 325). Therefore, despite the dynamics of the DO probe and the stir, Equation 2.12 is the fastest available way to calculate OTR. The problem is the unknown coefficient α, which represents all the slowly changing factors in k_La. To find α, Equation 2.3 can be modified as if the off-gas sensor measures the gases at the liquid surface directly without any delay as shown in the equation

$$OTR_{off-gas-SL} = F_r(b_{in} - b_{SL}) \tag{2.13}$$

where b_{SL} and $OTR_{off-gas-SL}$ denote oxygen concentration at the liquid surface level and the oxygen transfer rate computed using off-gases measured instantaneously at the liquid surface level. This change was made so that the following expression can be used

$$OTR = OTR_{off-gas-SL}$$

$$k_La \cdot DF = F_r(b_{in} - b_{SL})$$

$$b_{SL} = b_{in} - \alpha \cdot \frac{N \cdot DF}{F_r} \tag{2.14}$$

and find out the unknown parameter α. To find out the unknown coefficient α using Equation 2.14, the dynamics of bioreactor head space and off-gas sensor can be characterized in a state space linear time invariant system. Then an adaptive estimator is used to iteratively estimate the value of α.

2.2 Head Space and Off-Gas Sensor Dynamics

The bioreactor headspace dynamics can be written as a first order model

$$\dot{b_h} = \frac{1}{\tau_h}(b_{SL} - b_h) \tag{2.15}$$

where $\tau_h = \frac{V_h}{M_f}$ is the vessel headspace dilution time constant and it is changing slowly over the course of the fermentation run due to increasing in the culture liquid. Moreover, the M_f rate could change from one experiment to another. The off-gas sensor dynamics can also be characterized by a first order model

$$\dot{b_{out}} = \frac{1}{\tau_b}(b_h - b_{out}) \tag{2.16}$$

with a time constant τ_b that is almost constant and independent of M_f rates ranging from 1 to less than 8 [L/minute]. As a result, 55 seconds will be used for τ_b. Using Equation 2.15 and Equation 2.16, almost time in-varying linear system for the dynamics of bioreactor headspace and off-gas sensor could be written as

$$\begin{aligned} \dot{\bar{\mathbf{x}}} &= \bar{A}\bar{\mathbf{x}} + \bar{B}\bar{f} \\ \mathbf{y} &= \bar{C}\bar{\mathbf{x}} \end{aligned} \tag{2.17}$$

$$\bar{\mathbf{x}} = \begin{bmatrix} b_h \\ b_{out} \end{bmatrix}, \quad \bar{A} = \begin{bmatrix} -\tau_h^{-1} & 0 \\ \tau_b^{-1} & -\tau_b^{-1} \end{bmatrix}, \quad \bar{B} = \begin{bmatrix} b_{in} & \alpha \\ 0 & 0 \end{bmatrix},$$

$$\bar{C} = [0\ 1], \quad \bar{f} = \tau_h^{-1} \cdot \begin{bmatrix} 1 \\ \frac{-N \cdot DF}{F_r} \end{bmatrix}$$

2.3 Design of α Adaptive Estimator

Equation 2.17 has an unknown coefficient α in the matrix $\bar{B}$, and now, we need an adaptive estimator for this unknown coefficient. We start designing the adaptive estimator by finding the

system's transfer function,

$$\bar{G}(s) = \bar{C}(sI - \bar{A})^{-1}\bar{B} = \frac{\tau_b^{-1}}{\mathbf{s}^2 + (\tau_h^{-1} + \tau_b^{-1})\mathbf{s} + \tau_h^{-1} \cdot \tau_b^{-1}} \begin{bmatrix} b_{in} & \alpha \end{bmatrix} \tag{2.18}$$

so that the system matrices are rewritten in the observable canonical form, as a requirement of the implemented estimator [Kudva and Narendra, 1973, Narendra and Annaswamy, 2012]. As a result, the observable canonical form realization of Equation 2.17 is

$$\begin{aligned} \dot{\mathbf{x}} &= A\mathbf{x} + Bf \\ \mathbf{y} &= C\mathbf{x} \end{aligned} \tag{2.19}$$

$$\mathbf{x} = \begin{bmatrix} b_{out} \\ b_h \end{bmatrix}, \quad A = \begin{bmatrix} -(\tau_h^{-1} + \tau_b^{-1}) & 1 \\ -(\tau_h^{-1} \cdot \tau_b^{-1}) & 0 \end{bmatrix}, \quad B = \begin{bmatrix} 0 & 0 \\ b_{in} & \alpha \end{bmatrix}$$

$$C = [1 \;\; 0], \quad f = \begin{bmatrix} f_1 \\ f_2 \end{bmatrix} = \begin{bmatrix} \tau_h^{-1} \cdot \tau_b^{-1} \\ \frac{-\tau_h^{-1} \cdot \tau_b^{-1}}{F_r} \cdot N \cdot DF \end{bmatrix}$$

As an assumption required by the implemented estimator, **first**, the system matrix A must be stable, and this is satisfied by Equation 2.18, where the real parts of the system poles are less than zero. So, the system is BIBO stable. **Second**, $C^T(sI - A)^{-1}d$ must be strictly positive real, where $d = [1 \; d_2]^T$ and d_2 will be chosen later in this chapter based on this assumption and to meet other design requirements as well.

Equation 2.19 has the unknown parameter α in the B matrix, and now we build the adaptive estimator to find an estimated value $\hat{\alpha}$ of the unknown parameter. We define the estimator state variables in the vector $\mathbf{z}$

$$\mathbf{z} = \begin{bmatrix} \hat{b_{out}} \\ \hat{b_h} \end{bmatrix}$$

and using the system matrices A and B in Equation 2.19, the adaptive estimator is built as shown below

$$\dot{\mathbf{z}} = A\mathbf{z} + \hat{B}f + \mathbf{M}, \tag{2.20}$$

where $\hat{B}$ is the system B matrix in observable canonical form with the estimated unknown parameter

$\hat{\alpha}$. $\mathbf{M}$ is an adaptive auxiliary vector input

$$\mathbf{M} = \begin{bmatrix} 0 \\ -\mathbf{e}\zeta^{\mathbf{T}}\mathbf{\Lambda}\mathbf{A_2}\zeta \end{bmatrix}$$

where $\mathbf{\Lambda}$ is a gain diagonal positive definite matrix.

$$\mathbf{\Lambda} = \begin{bmatrix} \Lambda_{11} & 0 \\ 0 & \Lambda_{22} \end{bmatrix}, \tag{2.21}$$

and ζ is

$$\zeta = \mathbf{G}(\mathbf{s}) \cdot f_2,$$

which is obtained by passing the system input f_2 through an auxiliary signal generating filter bank

$$\mathbf{G}(\mathbf{s}) = \begin{bmatrix} \frac{s}{s+d_2} \\ \frac{1}{s+d_2} \end{bmatrix},$$

$d_2 = 8.3 \times 10^{-3}$, which is chosen; **first** to meet the assumption $C^T(sI - A)^{-1}d$ is strictly positive real, and, **second**, based on the system sampling time. That is because the estimator is designed in continuous time but it is implemented in discrete time, the pole of $\mathbf{G}(\mathbf{s})$ is chosen such that it is at least a factor of 25 smaller than the sample time $\frac{2\pi}{15}$ [rad/sec] [Franklin et al., 2011]. The estimator error $\mathbf{e}$ is

$$\mathbf{e} = \hat{b_{out}} - b_{out}, \tag{2.22}$$

and $\mathbf{A_2}$ is

$$\mathbf{A_2} = \begin{bmatrix} 0 & -d_2 \\ 0 & 1 \end{bmatrix}$$

The adaptive law is

$$\dot{\hat{\alpha}} = -\mathbf{e}S\mathbf{\Lambda}\zeta \tag{2.23}$$

which updates the estimated unknown coefficient $\hat{\alpha}$, where $S = [0 \;\; 1]$ is to convert the vector $\mathbf{\Lambda}\zeta$ into a scaler. Then, after $\hat{\alpha}$ is found, the estimated oxygen transfer rate $\widehat{OTR}$ and estimated oxygen

uptake rate $\widehat{OUR}$ are calculated by

$$\widehat{OTR} = \hat{\alpha} \cdot N \cdot DF \tag{2.24}$$

$$\widehat{OUR} = \widehat{OTR} - \dot{C} \tag{2.25}$$

The iterative algorithm can be found in Appendix B.

2.4 Computing the Expected O_2 Mole Ratio in the Sparge Air

The idea of tracking the states of the system especially $\widehat{OUR}$ using off-gas sensor is to compare the measured ratio of O_2 at the output with the ratio of O_2 in the sparge air. The difference between the two values is actually the demand of O_2. In some bioreactors, gas mixing is controlled by a digital control unit DCU via solenoids. As shown in Figure 2.3, when Gasmx signal is 0%, no O_2 will flow to the sparger, but when Gasmx is 10%, air solenoid is opened for nine seconds and O_2 solenoid is opened for one second. The ratio of O_2 in the sparge air could be computed and it is vital to assure the accuracy of the computation. When solenoids are used to mix input gases, then the equation

$$b_{in} = \frac{(100 - GasMx) \cdot b_{air} \cdot M_{f-air} + GasMx \cdot M_{f-O_2} \cdot C_f}{100 \cdot M_f} \tag{2.26}$$

is used to compute the mole ratio of O_2 in the sparge air using compressed air and O_2 from a tank, where b_{air}, M_{f-air}, and M_{f-O_2} are oxygen mole ratio in air, mass flow rate of air, and mass flow rate of oxygen, respectively. C_f is Correction factor of M_f meter measurement when measuring mass flow of pure oxygen. For our specific system, the value of C_f could be calculated by

$$C_f = (\frac{S_{current}}{S_{new}})^{0.3} \tag{2.27}$$

where $S_{current} = 1$ is the specific gravity of original calibration gas (air), and $S_{new} = 1.1044$ is specific gravity of new gas (O_2). $C_f = 0.9706$ for oxygen. Equation 2.27 can be found in the

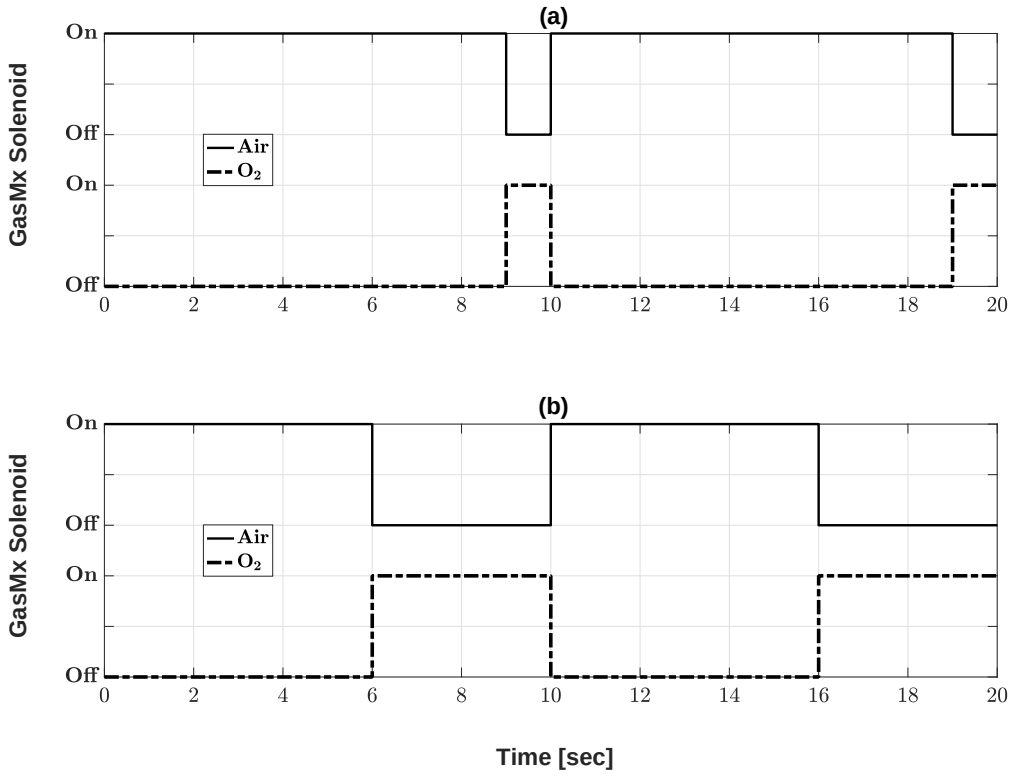

Figure 2.3: DCU solenoid period and duty cycle. **(a)** 10% DCU GasMx signal results in 28.57% oxygen concentration in sparge air. **(b)** 40% DCU GasMx signal results in 51.40% oxygen concentration in sparge air.

MFM user's guide for mass flow meter model number FLR 1000 by Omega. C_f is required in the calculation because we use the same M_f meter to balance the air and O_2 so that they read the same mass flow rate.

2.5 Tuning and Balancing the Sparge Gases

The calculation of the $OTR_{off-gas-SL}$ requires an accurate calculation of the oxygen mole ratio b_{in} in the sparge air. At the steady state and when there is no consumption of oxygen in the bioreactor, the off-gas measurements of O_2 should be equal to the calculated b_{in}. In the proposed system configuration Figure 2.1, only one mass flow meter MFM is used. It is assumed to not have instant time response as was the case for the experimental setup, where the time response $t_{67}\%$ was about 30 seconds (specified by the manufacturer, Engineering Inc., for the gas mass flow meter

Omega FLR 1000). Therefore, to use only one MFM and to cancel the impact of the time response, Equation 2.26 is valid only when M_{f-O_2} and M_{f-air} are tuned and balanced. Under this condition, each gas line, when fully open at 100%, gives the same reading measured by M_f meter located just before the bioreactor sparger, see Appendix A for balancing and tuning procedure. When the expression

$$M_{f-air} = M_{f-O_2} = M_f \tag{2.28}$$

is satisfied, then Equation 2.26 could be rewritten as

$$b_{in} = \frac{(100 - GasMx) \cdot b_{air} + GasMx \cdot C_f}{100} \tag{2.29}$$

An experiment was don (called Experiment 58) to validate results of Equation 2.29. The system was configured as shown in Figure 2.1 and the two lines of compressed air and O_2 were tuned so that every line gives the same mass flow rate when the line is opened 100% using the signal $GasMx$. The bioreactor vessel had water without biomass to have zero oxygen demand. The signal $GasMx$ was incremented every 20 minutes by five. Table 2.2 shows the expected oxygen mole ratio, that should be measured by the off-gas sensor at the exhaust, calculated by Equation 2.29 for two cases: $C_f = 1$ ignoring the correction factor that should be accounted for when measuring pure oxygen by the MFM, and $C_f = 0.9706$ considering the pure oxygen as the gas being measured by the MFM.

GasMx%	**Expected measurements by off-gas sensor at zero O_2 demand**	
	With M_f balanced and $C_f = 0.9706$	**With M_f balanced and $C_f = 1$**
0	0.2096	0.2096
5	0.24765	0.24912
10	0.2857	0.28864
15	0.32375	0.32816
20	0.3618	0.36768
25	0.39985	0.4072
30	0.4379	0.44672
35	0.47595	0.48624
40	0.514	0.52576

Table 2.2: GasMx% and expected measurements by off-gas sensor.

Figure 2.4 shows the results of experiment 58. When $C_f = 1$, there was an error between the expected and the measured oxygen mole ratios. The error increases with higher $GasMx$ oxygen

enrichment levels. When $C_f = 0.9706$, however, the expected and measured oxygen mole ratio were almost the same despite the delay caused by the head space dilution and the off-gas sensor time response. Note that, Equation 2.29 gives accurate expected measurements for GasMx values less than 50% which is the maximum safe limit of the off-gas sensor used in our system.

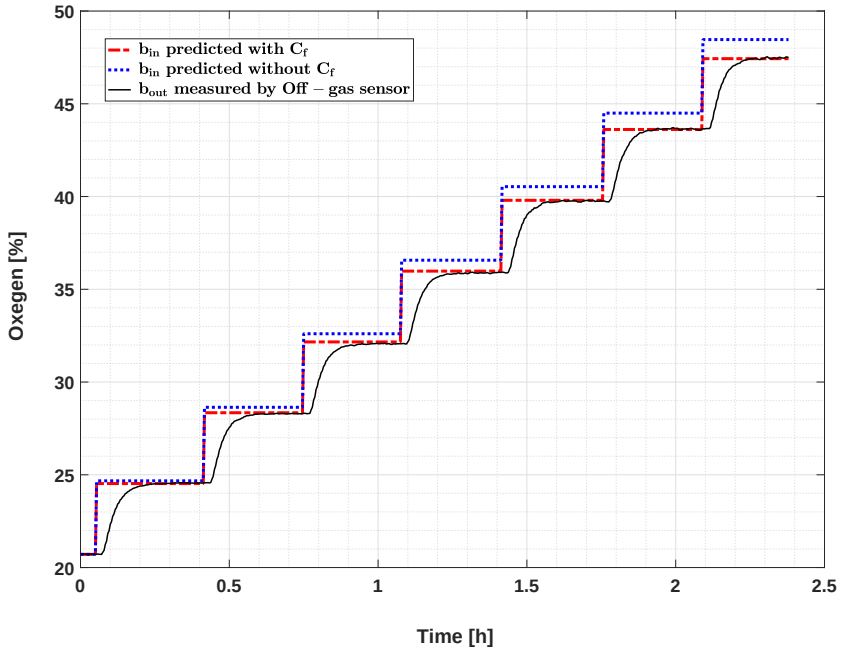

Figure 2.4: Calculated V.S. measured oxygen mole ratios at input and output at zero oxygen demand. The oxygen mole ratio at the input b_{in} was calculated with the mass flow meter Correction factor C_f as shown in red color. This calculation gave an accurate results at different oxygen enrichment concentrations when compared to the oxygen mole ratio measured by the off-gas sensor at the output b_{out} when there was no cells in the bioreactor and the oxygen demand was zero. However, there was an error in b_{in} when computed without C_f.

2.6 Further Considerations

2.6.1 PI-controlled dissolved oxygen

A Zig-Zag controlled DO was suggested by [Wang, 2014] mainly to provide a sufficient excitation for the estimator. However, using a PI controller, which is embedded in the bioreactor control unit DCU is preferred over the Zig-Zag due to the following reasons:

A. The PI controller is well adopted by industry due to robustness and reliability.

B. Experimentally, the PI controller can provide a sufficient excitation for the estimator.

C. Kalman filters can be used to filter out noise caused by PI controlled DO.

D. The PI controller is more robust than the Zig-Zag especially during probing times at high oxygen demand when the biomass becomes large and when OTR is close to maximum hardware limits; i.e., stir speed is near 1200 rpm or off-gas measurement of O_2 is 50%. For our particular system, in other words, the fastest response of the Zig-Zag controller is two times the sampling time ($30s$), which is much longer than the DCU sampling time. Therefore, the DCU PI controller is much faster and thus reliable.

E. The PI controller gain tuning is very common in the literature and there are many suggested solutions such as gain-scheduling approach [Åkesson and Hagander, 1999] or continuous identification of gains [Kumar et al., 2008, Pramod and Chidambaram, 2000, Ertunc et al., 2009].

F. The Zig-Zag method of controlling the DO level can cause perturbations to the oxygen demand that is made by the biomass respiration. This causes wrong calculations of $\widehat{OTR}$ and $\widehat{OUR}$.

Therefor, the DCU PI controller will be used for controlling the DO level.

2.6.2 Variable gain for the adaptive estimator

The modified estimator explained in Section 2.3 was tested with recorded data of previous experiments. The purpose was to tune the estimator gain and to make sure of the performance of the new modifications, which are using only one unknown parameter α and scaling C^* by the ratio $\frac{b_{in}}{b_{air}}$. The estimator performance was highly dependent on the values of the gain matrix Λ. Large gain values help for a faster convergence but cause a huge amplification of the estimator error. This usually causes the estimator output to blow up. Small gain values, on the other hand, cause the estimator to very slowly converge to the correct value but to preform much better at later times of a fermentation run when OTR is high.

By using data from previous experiments, it was required to have a decreasing gain along the course of the fermentation run. To have such a decreasing gain, it is required to have a smoothly increasing or decreasing variable among the process parameters. One of the best parameters that could be utilized here is the estimated liquid volume so that the estimator gain becomes a function of the estimated liquid volume. An example of the estimated liquid volume from one of the experiments

is shown in Figure 2.5 and the proposed gain, which is obtained by trial and error using data from previous experiments, is

$$\Lambda_{11} = \Lambda_{22} = \frac{300}{V^{14}} + 0.01 \tag{2.30}$$

where $V = V_c$ is the total liquid volume. This is estimated by summing the volume of initial liquid plus volumes of the base and feed pumped into the culture liquid during the cultivation. The output of Equation 2.30 , which is plotted in Figure 2.6, is used for both entries of the diagonal gain matrix Λ.

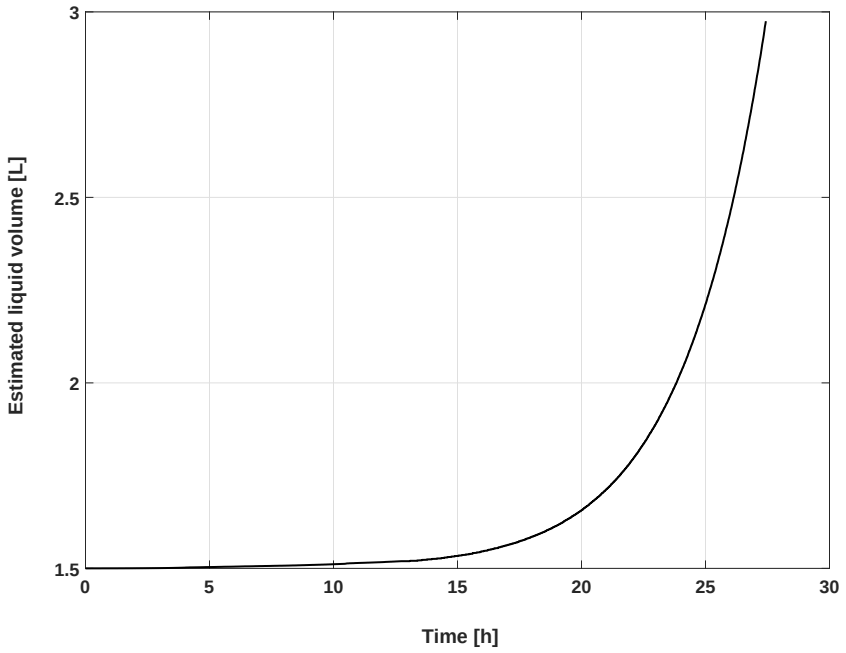

Figure 2.5: Estimated liquid volume.

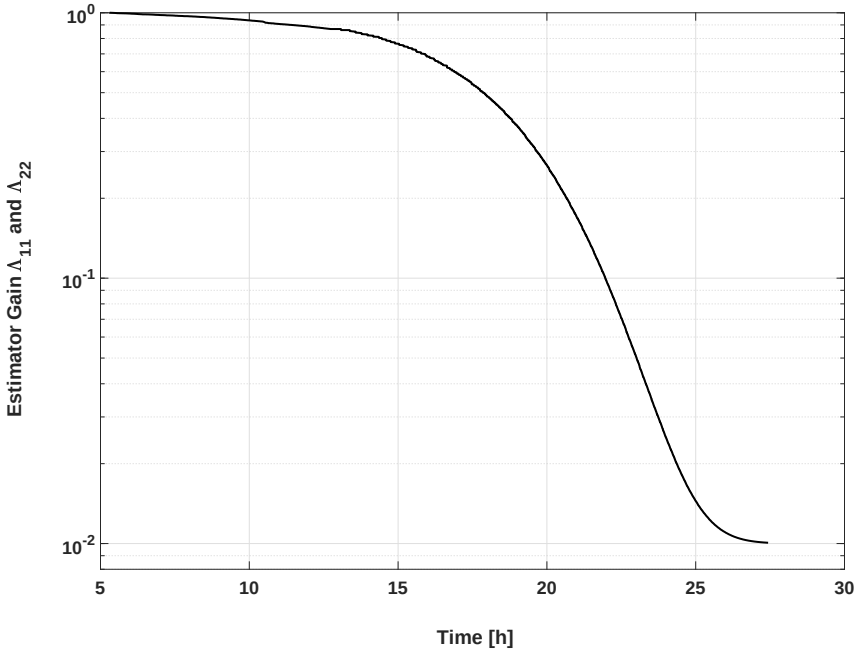

Figure 2.6: Proposed estimator gain as a function of estimated liquid volume.

Chapter 3

Results and Discussion

Two *E.coli* fermentations were controlled using the proposed OTR estimator with oxygen enriched air. These cultures reached high-cell densities typical of industrial fermentations. Observation regarding the estimator will be discussed toward further refinement.

For all details regarding the different settings and conditions of all experiments used in this chapter, see Appendix C.

3.1 Exponential Feeding Profile (μ_{set})

Exponential feeding (μ_{set}) is one common method used in industry and also in research laboratories to conduct fed-batch cultures of *E.coli* in order to reach high-cell densities. The estimator was first tested with real-time data collected from an experiment (called Experiment 60) for *E.coli* MG1655 cultured grown with an exponential feeding profile and oxygen enriched air. The purpose of this test was to probe the estimator performance under oxygen enriched air. As shown in Figure 3.1, $\widehat{OTR}$ is superimposed on $OTR_{off-gas}$ that increased along the cultivation time without downward shifting after each increase in the oxygen enrichment. $\widehat{OTR}$ converged to $OTR_{off-gas}$ in about seven hours, as shown in Figure 3.2(a), after the inoculation with *E.coli* cells. The decrease in both $\widehat{OTR}$ and $OTR_{off-gas}$ at 7.8 [hours] was due to the end of batch phase. The spikes in $OTR_{off-gas}$ appear after every transition in GasMx signal and this is because the term b_{in} in Equation 2.26 instantaneously changes with GasMx signal, and b_{in} is used in both $\widehat{OTR}$ and $OTR_{off-gas}$ calculations, with Equation 2.24 and Equation 2.3, respectively.

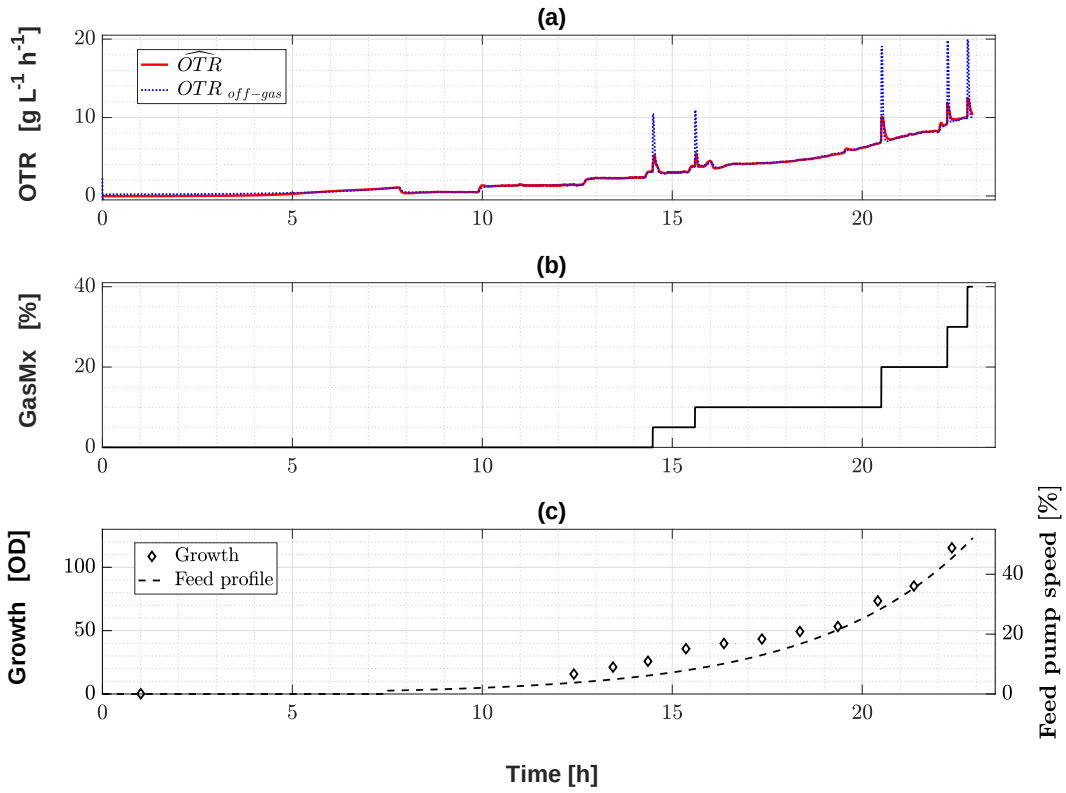

Figure 3.1: Exponential feed profile. (a) shows the estimated oxygen transfer rate $\widehat{OTR}$ in red color superimposed on blue colored $OTR_{off-gas}$, which is calculated using off-gas measurement of O_2. (b) shows the oxygen enrichment signal (GasMx). (c) shows optical density measurements by a spectrophotometer and the feed rate, where 100% corresponds to 5.7 [mL/min].

Then, $OTR_{off-gas}$ takes a few minutes to return to its previous value due to the system total time constant, and $\widehat{OTR}$ re-converges again as shown in Figure 3.2(b).

3.2 BOOM II

BOOM controller was first proposed by [Pepper, 2015]. Then the algorithm was modified (BOOM II) by [Gharakozlou Lashkari, 2017]. The algorithm controls the feed rate so that the *E.coli* grows at near optimal growth rate with minimum acetate accumulation before and after induction.

Under feed-limited cultivation, theoretically, the culture respiration of oxygen should increase when the feed rate increases and the culture is in the oxidative metabolic state. If the

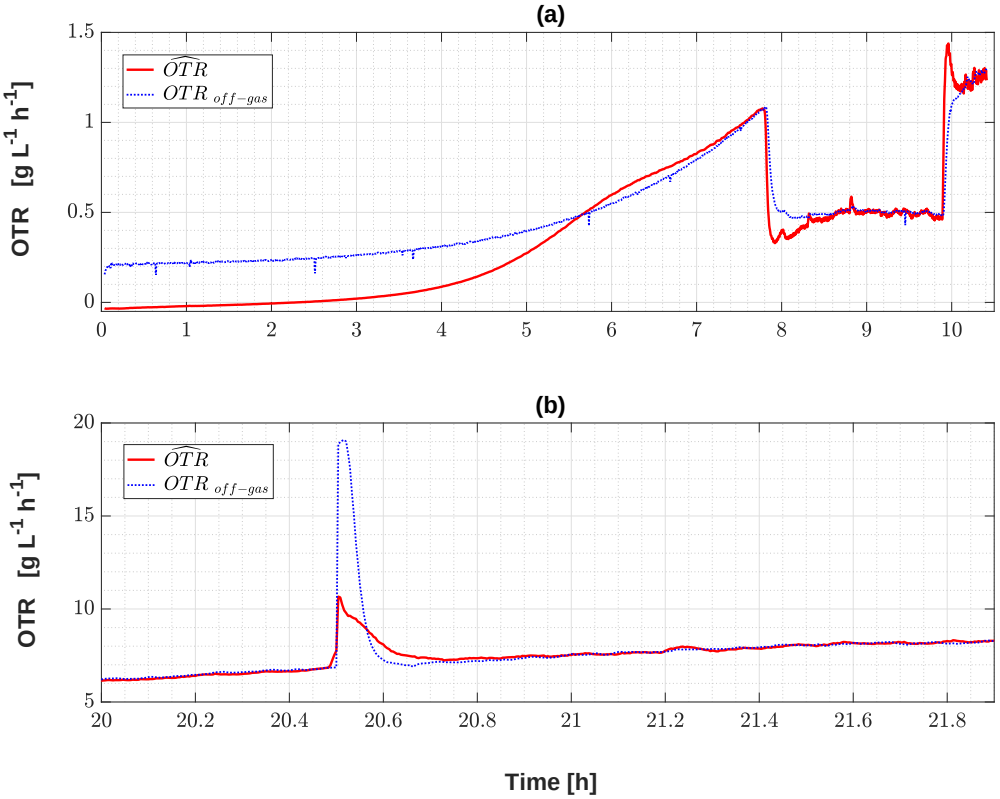

Figure 3.2: Exponential feed profile zoomed at two different time intervals. The estimated oxygen transfer rate $\widehat{OTR}$ in red color superimposed on blue colored $OTR_{off-gas}$, which is calculated using off-gas measurement of O_2. (a) shows the estimator converges to $OTR_{off-gas}$ after about 7 hours. (b) shows the estimator re-converges after an increase in the oxygen enrichment signal (GasMx).

increase in feed rate continues, the culture respiration of oxygen should start slowing down once the culture enters the overflow metabolism state or region. BOOM II algorithm is meant to keep the culture just under the overflow region. In summary, the BOOM II algorithm depends on $\widehat{OUR}$ and feed rate signals F. After the end of the batch phase, fed-batch starts with an initial feed rate $F_i = F_0$. Then, after a few minutes, the culture is probed to detect its metabolism state. The probe is done by increasing the feed rate exponentially for a few minutes. During this probing, a sensitivity ratio, which is computed by

$$SR = \frac{\frac{\dot{\widehat{OUR}}}{\widehat{OUR}}}{\frac{\dot{F}}{F}},$$

is monitored. The SR signal should increase and exceed certain threshold level if the culture is in the oxidative region. If the SR signal exceeds the threshold level and starts decreasing, then the

transition from the oxidative to overflow is detected and the probing stops. If the SR signal does not exceed the threshold level until a maximum specific probing time, then the culture is considered in the overflow region and the probing stops. A higher feed rate is set if the culture was considered to be in the oxidative region. Otherwise, the feed rate is decreased.

The estimator was used in an experiment (called Experiment 74) of *E.coli* MG1655 culture using BOOM II to control the feeding and to grow the culture at near optimal growth rate. In this experiment, the sparge air was enriched with oxygen to extend the OTR whenever the stir speed was approaching the maximum limit. Figure 3.3 shows both $\widehat{OTR}$ and $OTR_{off-gas}$ along with the oxygen enrichment signal (GasMx) during the whole cultivation time. The estimator provided the BOOM II controller with $\widehat{OTR}$, which was responding to the probing signal ahead of the $OTR_{off-gas}$, and thus enabling the BOOM II controller to quickly detect the metabolic state and change the feeding rate. Figures 3.4 and 3.5 show examples of $\widehat{OTR}$ which was expected ahead of $OTR_{off-gas}$ at different cultivation times. Figure 3.4(c) shows $\widehat{OTR}$ ahead of $OTR_{off-gas}$ during a probing time, which was followed by a spike in $OTR_{off-gas}$ due to an increase in the GasMx signal as explained previously in Section 3.1. The noise in the $\widehat{OTR}$ was due to gains tuning problem of the DO PI controller. The tuning problem becomes more apparent at higher values of k_La [Åkesson and Hagander, 1999].

3.3 Importance of Accurate Identification of Oxygen Mole Ratio in the Input Gas

The OTR calculations depend on the partial pressure of oxygen in the sparge air b_{in}. In our system, we have only one off-gas sensor which is connected to the exhaust of the bioreactor. As mentioned in Section 2.5, balancing the two input gases, air and O_2, is required so that every line provides the same flow rate.

To see the importance of the balancing, we can use the oxygen demand as a reference to compare between two different experiments (called Experiments 5 and 60, see Appendix C). The two experiments were open loop controlled with an exponential feed profile and oxygen enriched sparge air. The two gas lines were not balanced in experiment 5. In a feed controlled *E.coli* culture in a bioreactor, oxygen demand, however, should look like the feed profile as long as the culture is in the oxidative state and in healthy condition. For experiment 5, which was open loop controlled

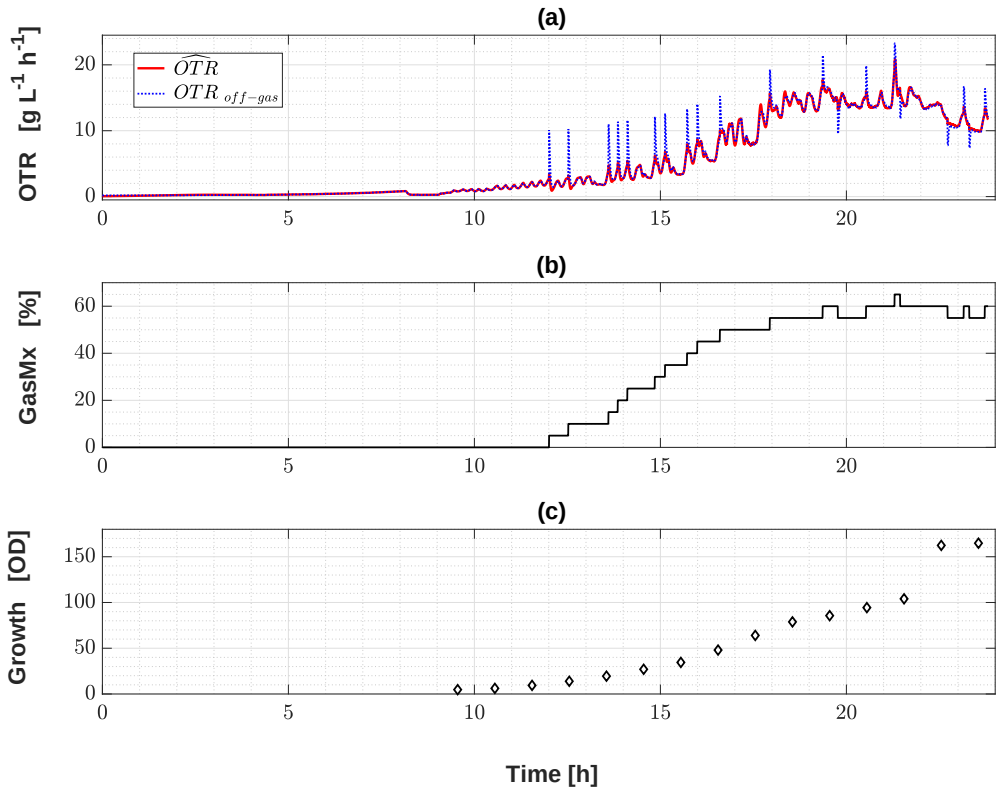

Figure 3.3: BOOM II feed controller. (a) shows the estimated oxygen transfer rate $\widehat{OTR}$ in red color superimposed on blue colored $OTR_{off-gas}$, which is calculated using off-gas measurement of O_2. (b) shows the oxygen enrichment signal (GasMx). (c) shows optical density measurements by a spectrophotometer.

with an exponential feed profile, Figure 3.6(a) shows the oxygen demand which looks like the feed profile but with downward shifting after every increase of the oxygen enrichment in the sparge air. Nevertheless, the culture was healthy according to many signals such as pH, CO_2, the total volume of base added to the culture, and the culture cell density measured by a spectrophotometer as shown in Figure 3.7(a), (b), (c), and (d), respectively.

$$O_{2-demand} = O_{2-in} - O_{2-out} \tag{3.1}$$

The demand is calculated by Equation 3.1, where O_{2-in} is the ratio of oxygen in the sparge air computed by Equation 2.29 but without balancing the mass flow rate of the air and oxygen lines, and without considering the correction factor ($C_f = 1$). O_{2-out} is the partial pressure of oxygen at the exhaust measured by the off-gas sensor. The reason of downward shifting in Figure 3.6 is due to

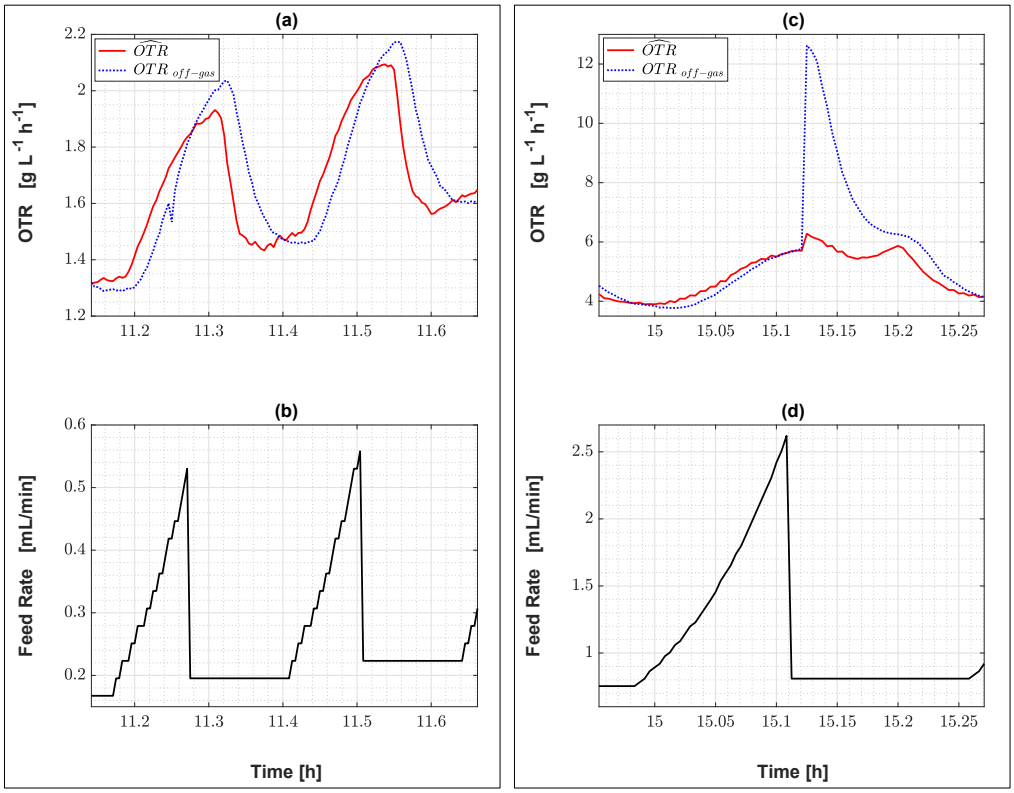

Figure 3.4: BOOM II Probing example 1 at different cultivation times. (a) and (c) show that the estimated oxygen transfer rate $\widehat{OTR}$ is a head of that calculated using off-gas measurements $OTR_{off-gas}$. (b) and (d) show exponentially increasing probing signal using 50% [v/v] Glucose solution. Note that, (a) and (c) show the $\widehat{OTR}$ response of the probing signal shown in (b) and (d), respectively.

wrong calculation of O_{2-in}. After increasing the oxygen enrichment in the sparge air, both O_{2-in} and O_{2-out} should increase with the same exact amount so that the oxygen demand stays at the same level as it was before increasing the level of oxygen enrichment.

O_{2-in} was always greater than what it should have been as shown in Figure 3.8. Table 3.1 summarizes Figure 3.8 and compares the oxygen demand before and after increasing the GasMx signal. It shows that the O_2 measurement of off-gas sensor was always greater than what was expected by calculation without balancing. This result indicates to a mass flow rate on O_2 line greater than the one on the line of air.

We can cancel the error by scaling down the off-gas sensor measurements of O_2 for every GasMx level. In other words, the off-gas sensor measurement was higher than what was expected for

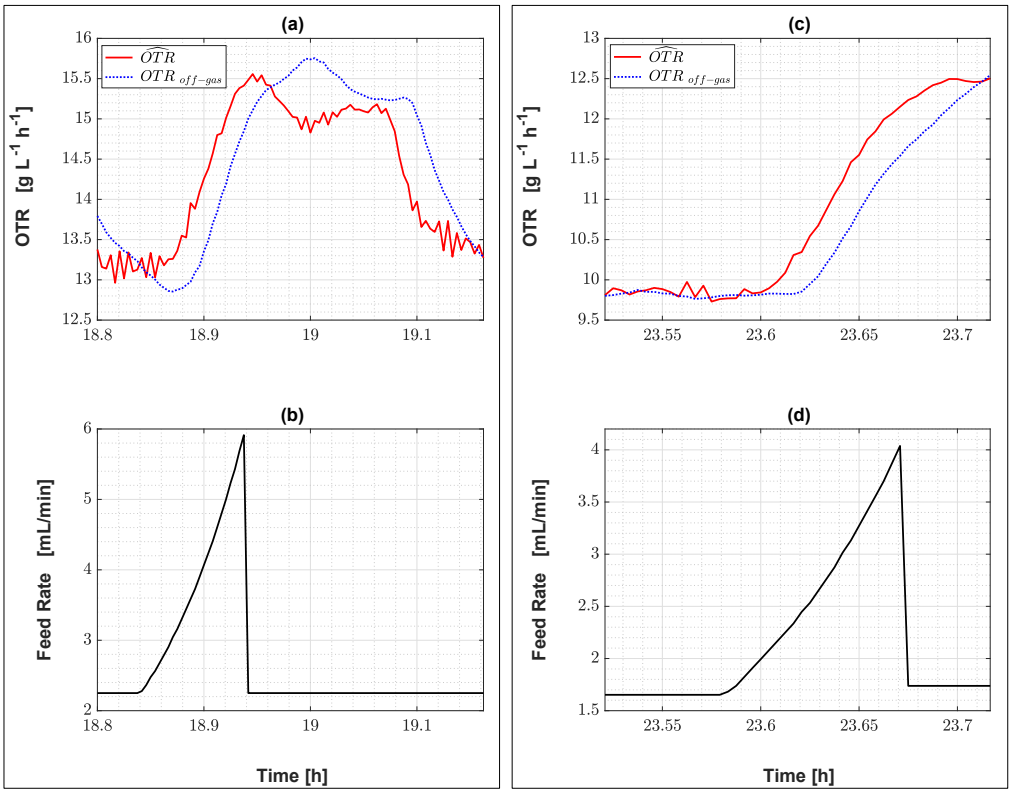

Figure 3.5: BOOM II Probing example 2 at different cultivation times. (a) and (c) show that the estimated oxygen transfer rate $\widehat{OTR}$ is a head of that calculated using off-gas measurements $OTR_{off-gas}$. (b) and (d) show exponentially increasing probing signal using 50% [v/v] Glucose solution. Note that, (a) and (c) show the $\widehat{OTR}$ response of the probing signal shown in (b) and (d), respectively.

GasMx [%]	**Unit**	**0**	**10**	**20**	**30**	**40**
Expected O_2 measurement at zero O_2 demand	$\frac{\text{mol}}{\text{mol}}$	0.2096	0.28864	0.36768	0.44672	0.52576
O_2 measurement before GasMx increase	$\frac{\text{mol}}{\text{mol}}$	-	0.175	0.2585	0.3302	0.3976
O_2 demand before GasMx increase	$\frac{\text{mol}}{\text{mol}}$	-	0.0346	0.03014	0.03748	0.04912
Expected O_2 measurements at current O_2 demand	$\frac{\text{mol}}{\text{mol}}$	-	0.25404	0.33754	0.40924	0.47664
O_2 measurement after GasMx increase	$\frac{\text{mol}}{\text{mol}}$	-	0.2759	0.35	0.4268	0.4921
Error	%	-	8.605	3.691	4.291	3.243

Table 3.1: Experiment 5, Off-gas sensor O_2 measurements with GasMx%.

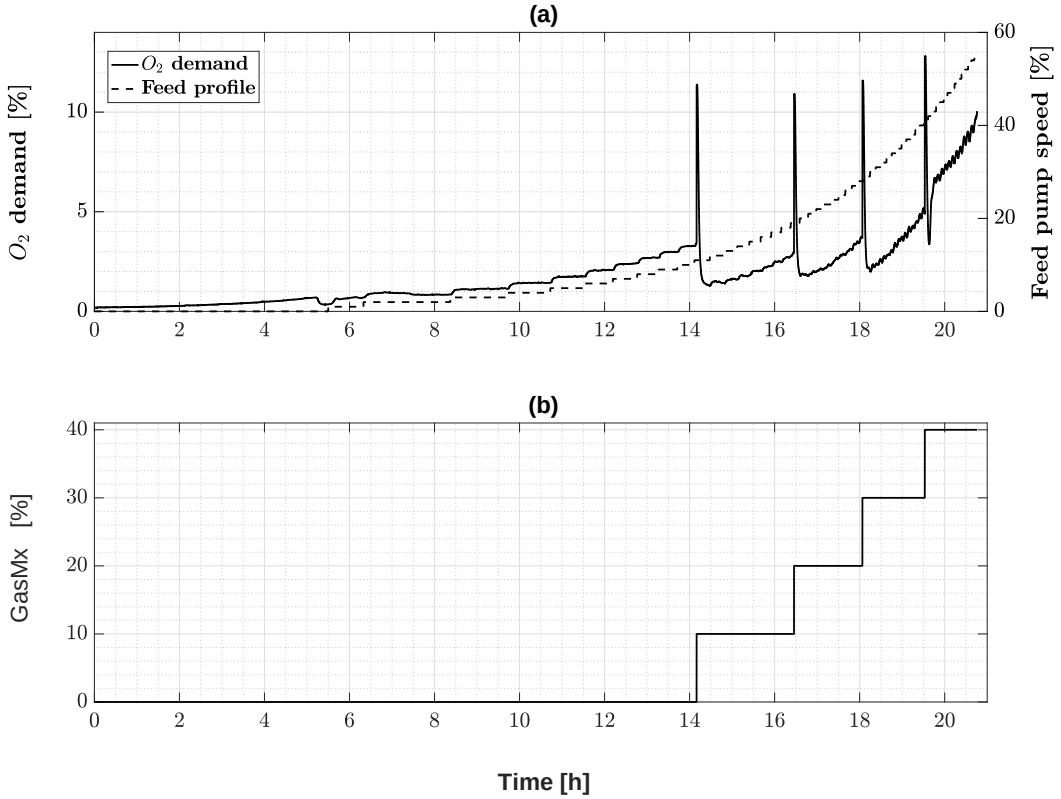

Figure 3.6: Experiment 5, O_2 demand. (a) shows the dotted line feed profile and the solid line O_2 demand shifting downward after every increase in the oxygen enrichment signal (GasMx), which is shown in (b).

GasMx (%)	**0**	**10**	**20**	**30**	**40**
Required scale down ratio	1	0.905	0.880	0.855	0.880

Table 3.2: Experiment 5 scale down ratios of O_2off-gas sensor measurements for different oxygen enrichment levels.

every GasMx level due to a higher mass flow rate of O_2 line. To cancel this error, only for discussion purpose, the off-gas sensor measurements of O_2 for every GasMx level can be scaled down so that the oxygen demand becomes equal before and after the change in oxygen enrichment level. Table 3.2 shows the ratios required to scale down every GasMx level so that the oxygen demand looks like the feed profile. Figure 3.9 shows the feed and corrected oxygen demand profiles. Figure 3.10(a) shows the $\widehat{OTR}$ when air and O_2 lines have unbalanced mass flow rates, and Figure 3.10(b) shows the $\widehat{OTR}$ after removing the error resulting from unbalanced mass flow rates of input gases.

In contrast, the two gas lines were balanced in experiment 60. Figure 3.11 shows $\widehat{OTR}$ and

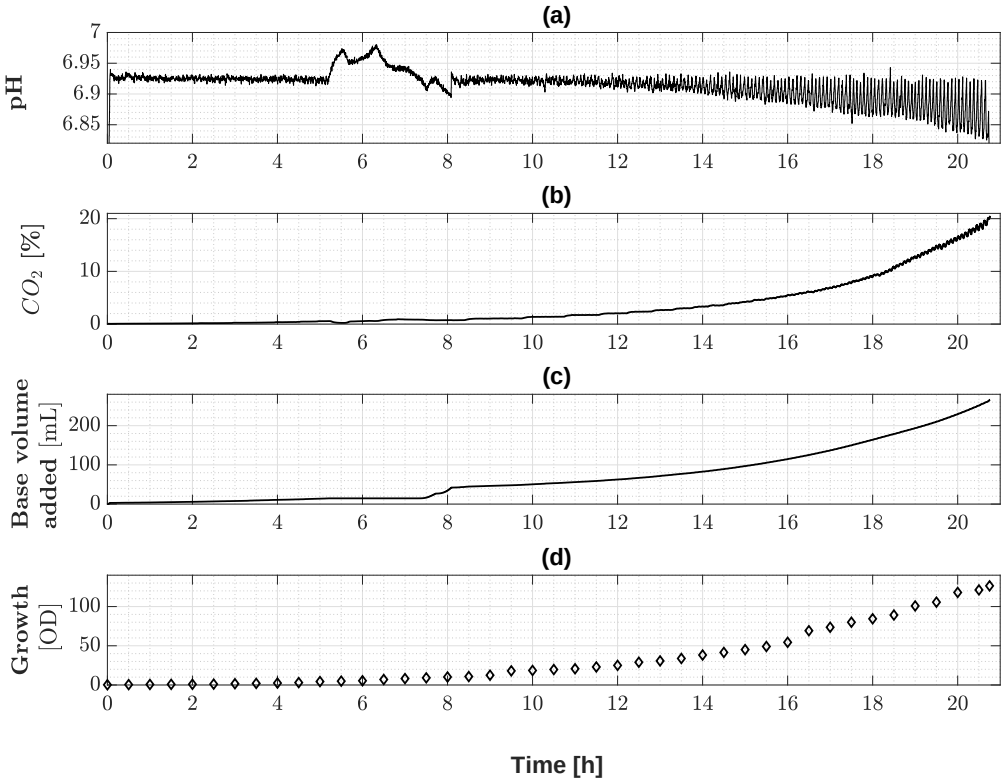

Figure 3.7: Experiment 5, *E.coli* growth indicators. (a) pH is regulated properly by the DCU. (b) CO_2 is increasing in the same pattern of the feeding profile, which is exponential. (c) Total volume of base added was also similar to the feeding profile. (d) shows optical density measurements by a spectrophotometer.

the oxygen demand which looks like the feed profile. Table 3.3, which summarizes Figure 3.12, shows the oxygen demand before and after increasing the GasMx signal in experiment 60. If we compare the average error in Tables 3.1 and 3.3, we can find a sufficient statistical evidence at $\alpha = 0.05$ level of significance to conclude that tuning and balancing the mass flow rate of the two input gases (air and O_2) has significantly reduced the error, which occurs when changing the oxygen enrichment level, in oxygen demand profile. Figure 3.13 shows experiment 60 signals: - pH, CO_2, total volume of base added to the culture, and the culture cell density measured by a spectrophotometer.

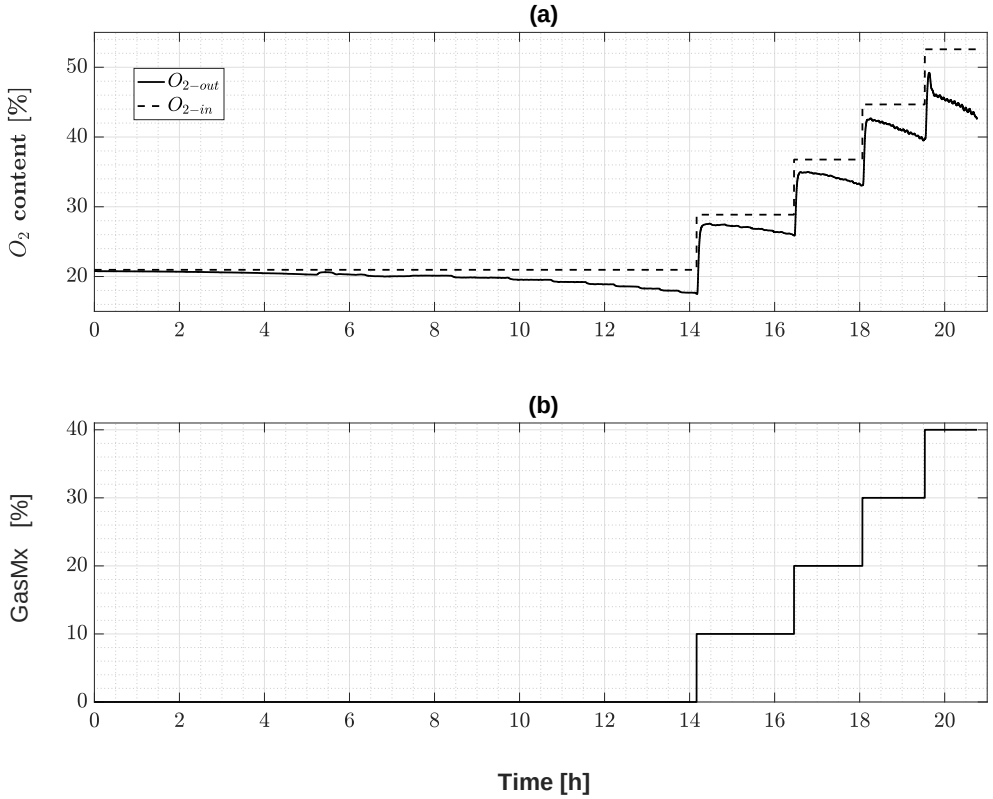

Figure 3.8: Experiment 5, oxygen mole ratio in input and output gases. (a) shows the expected oxygen mole ratio in the sparge air O_{2-in} and oxygen mole ratio measured by the off-gas sensor O_{2-out}. (b) shows the oxygen enrichment signal (GasMx).

GasMx [%]	**Unit**	**0**	**5**	**10**	**20**	**30**	**40**
Expected O_2 measurement at zero O_2 demand	$\frac{\text{mol}}{\text{mol}}$	0.2096	0.2476	0.2834	0.3597	0.4361	0.5124
O_2 measurement before GasMx increase	$\frac{\text{mol}}{\text{mol}}$	-	0.1935	0.2278	0.2403	0.2943	0.3622
O_2 demand before GasMx increase	$\frac{\text{mol}}{\text{mol}}$	-	0.0161	0.0198	0.0431	0.0654	0.0739
Expected O_2 measurements at current O_2 demand	$\frac{\text{mol}}{\text{mol}}$	-	0.2315	0.2635	0.3166	0.3707	0.4385
O_2 measurement after GasMx increase	$\frac{\text{mol}}{\text{mol}}$	-	0.2329	0.2654	0.318	0.3691	0.4383
Error	%	-	0.583	0.702	0.442	-0.431	-0.045

Table 3.3: Experiment 60, Off-gas sensor O_2 measurements with GasMx%.

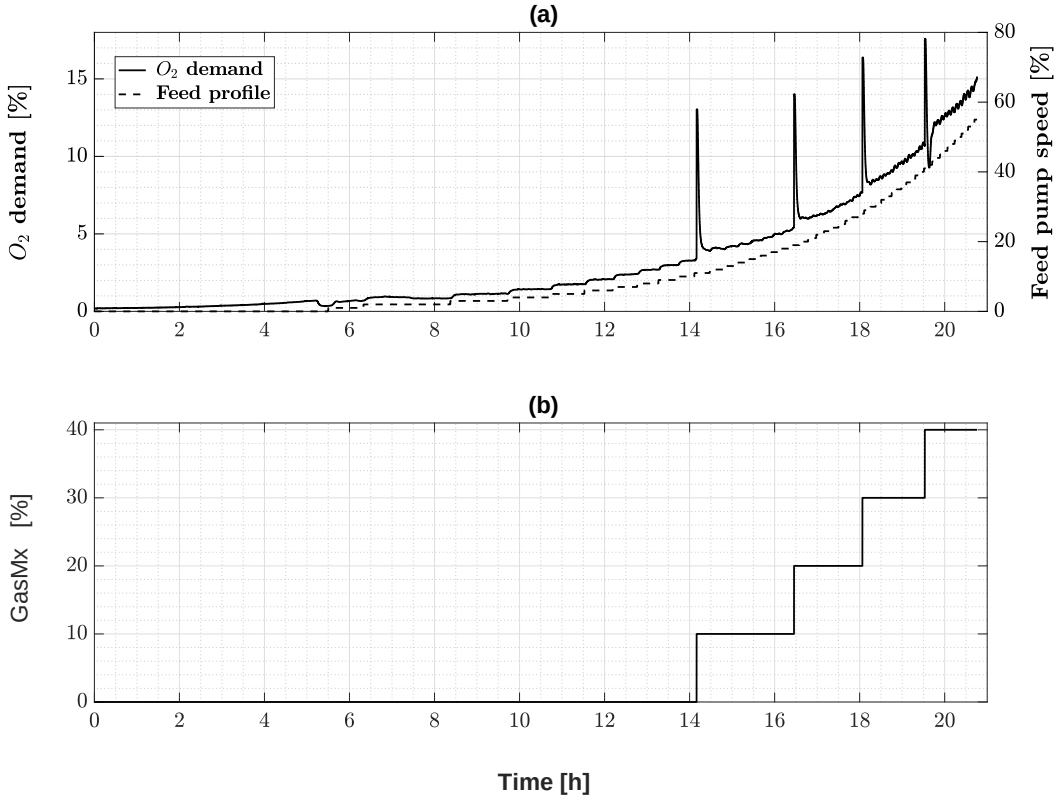

Figure 3.9: Experiment 5, corrected O_2 demand. (a) shows the dotted line feed profile and the solid line O_2 demand corrected using ratios in Table 3.2. (b) is the GasMx signal.

3.4 Some Observations and Suggested Improvements

3.4.1 Need for an adaptive gain

In Equation 2.30, which was

$$\Lambda_{11} = \Lambda_{22} = \frac{300}{V^{14}} + 0.01,$$

the gain was expressed as a function of total liquid volume and tuned by trial and error using data from many experiments with *E.coli* MG1655 culture. While this gain function worked well for many experiments, there will be still a need for a better tuning if another stain of *E.coli* cells is used. Another reason for the need of such an adaptive gain is if the system sampling time were changed due to a change in d_2 value, for example, then another tuning of Equation 2.30 will be needed. The liquid volume, moreover, is estimated based on feed and base rates of pumps and size of tubings.

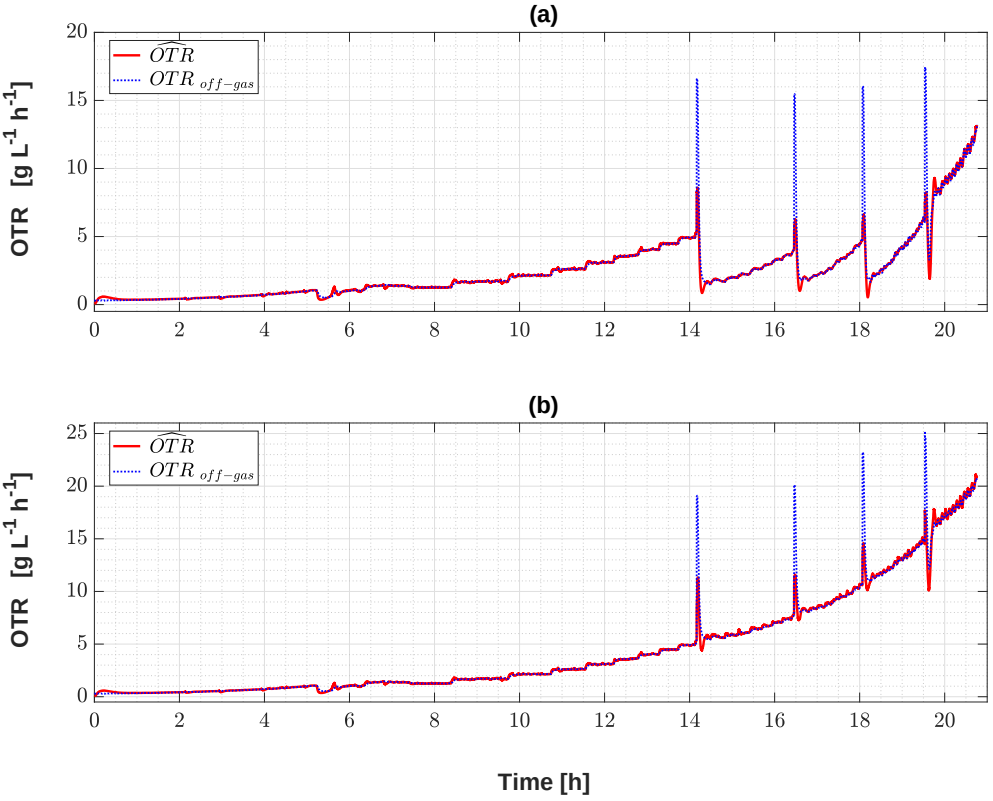

Figure 3.10: Experiment 5, $\widehat{OTR}$ and $OTR_{off-gas}$ after numarically correcting the oxygen demand. The estimated oxygen transfer rate $\widehat{OTR}$ in red color superimposed on blue colored $OTR_{off-gas}$, which is calculated using off-gas measurement of O_2. (a) shows the shifting in $\widehat{OTR}$ and $OTR_{off-gas}$ caused by mis-tuning of air and O_2 lines. (b) shows $\widehat{OTR}$ and $OTR_{off-gas}$ after scaling the the oxygen demand using the ratios in Table 3.2.

If the estimated value of the liquid volume changed, another tuning of the function gain will be required. The calculation of estimator gain as a function of culture volume might be subject to any flaw in the control part. For example, when the culture is in overflow metabolic state, more base is pumped into the culture, or when a probing lasts for a longer time, more glucose is pumped in. Then, by Equation 2.30, the estimator gain changes faster than what it should be.

Therefore, there is no such known independent variable that could be reliably used to calculate the estimator gain and thus an adaptive gain should be used for more accuracy and stability.

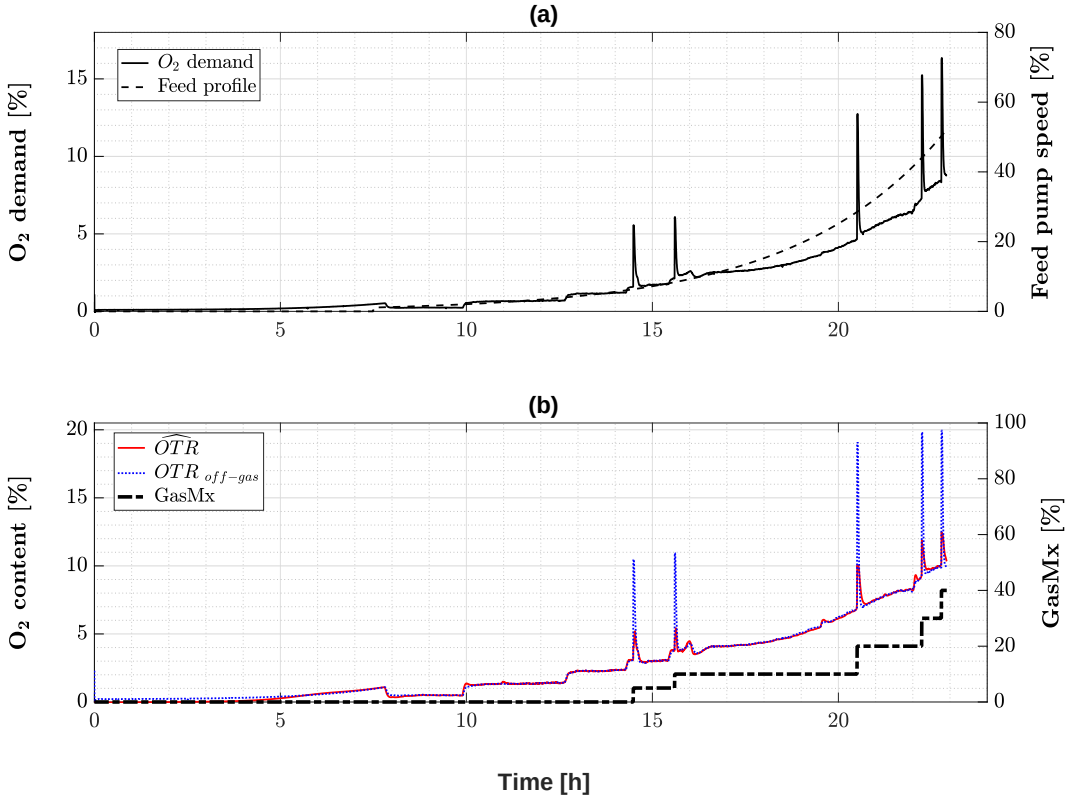

Figure 3.11: Experiment 60, cultivation profile. (a) shows the solid black colored O_2 demand and feed profile in dashed black color. (b) shows the dotted black colored GasMx signal along with the estimated oxygen transfer rate $\widehat{OTR}$ in red color superimposed on blue colored $OTR_{off-gas}$, which is calculated using off-gas measurement of O_2.

An adaptive gain could be obtained by

$$\dot{\mathbf{\Lambda}} = -\mathbf{\Lambda}\zeta\zeta^{\mathbf{T}}\mathbf{\Lambda} \tag{3.2}$$

and $\mathbf{\Lambda}$ is initialized as in Equation 2.21 [Narendra and Annaswamy, 2012]. Then Equation 2.23 could be rewritten as

$$\dot{\hat{\alpha}} = -\mathbf{e}F_g S\mathbf{\Lambda}\zeta \tag{3.3}$$

where F_g is a fixed positive gain. This adaptive gain was tested using data from many experiments. The estimator performance using the adaptive gain was almost similar to that using the function gain Equation 2.30. An example of the estimator performance using the adaptive gain with data of experiment 74 is shown in Figure 3.14, which shows that the estimator performs almost the same

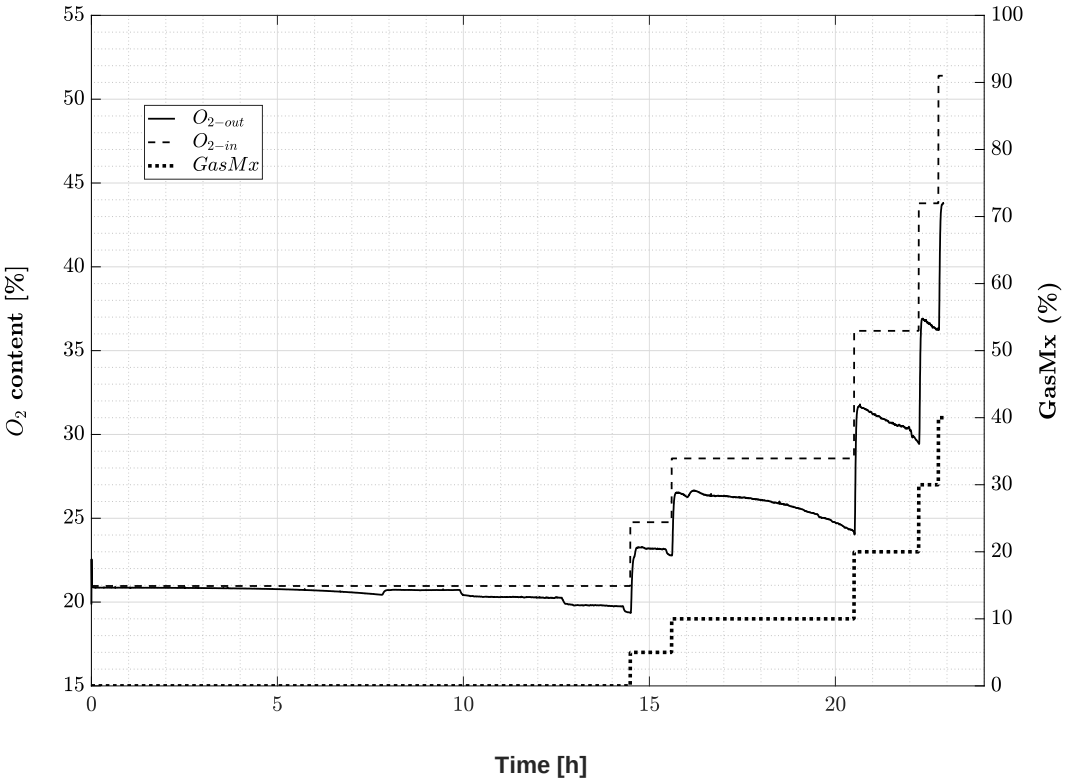

Figure 3.12: Experiment 60, oxygen mole ratio in input and output gases. The dashed line is the expected oxygen mole ratio in the sparge air O_{2-in} and the solid line is the off-gas sensor measurement of oxygen concentration at the reactor exhaust O_{2-out}. The dotted line is the oxygen enrichment signal (GasMx).

using either gains and $\widehat{OTR}$ is ahead of $OTR_{off-gas}$.

3.4.2 Persistent excitation

A better understanding of system excitation is still needed for faster convergence. However, it was observed that external excitation, such as Zig-Zag used in [Wang, 2014], is needed when the biomass is very small and the oxygen demand is very low. By looking at the data of different experiments, it was noticed that the estimator converges when the off-gas sensor starts measuring a decrease in O_2 value. For example, we usually start experiments with only air as the input gas which is measured 20.96% at the exhaust. The estimator usually converges when this measurement drops (due to oxygen demand of biomass or Zig-Zag C controller) to 20.92%. After the estimator converges and when oxygen demand is continuously increasing, a PI controller is recommended to be

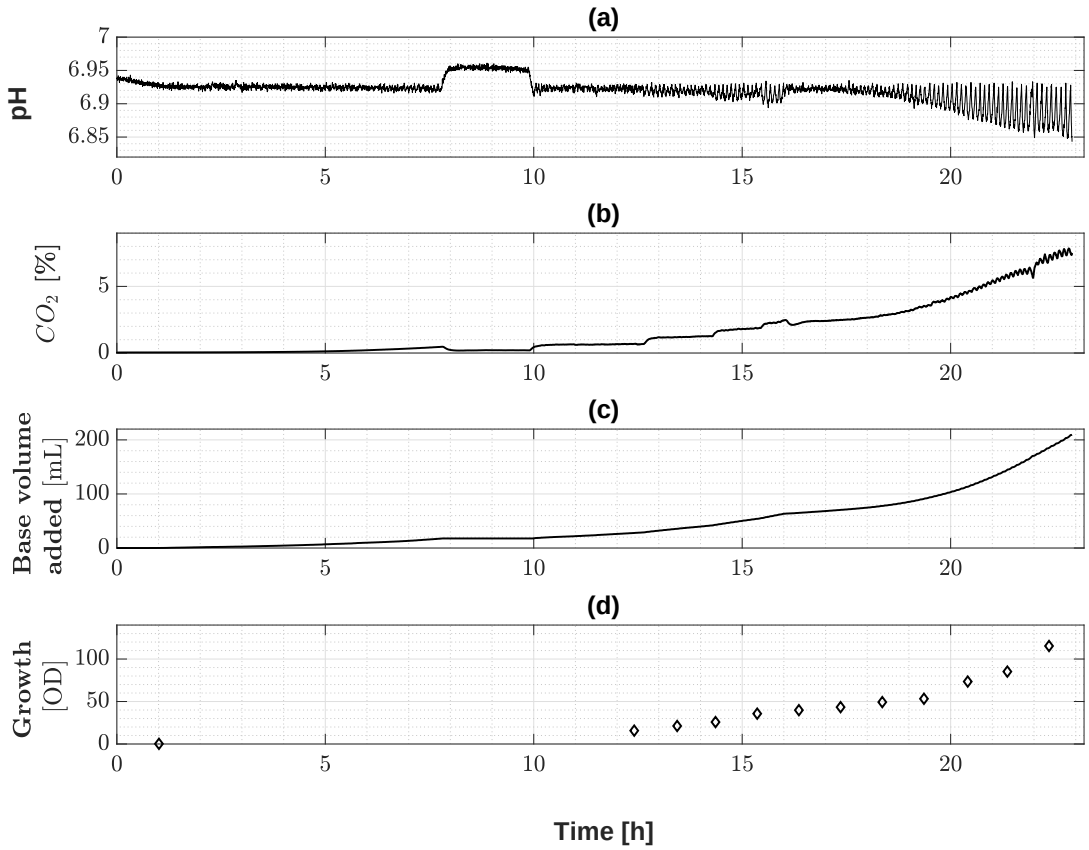

Figure 3.13: Experiment 60, *E.coli* growth indicators. (a) pH is regulated properly by the DCU. (b) CO_2 is increasing in the same pattern of the feeding profile, which is exponential. (c) the total volume of base added was also similar to the feeding profile. (d) shows optical density measurements by a spectrophotometer.

used for controlling C so that a better OUR estimation and more control robustness are achieved.

The input of the headspace linear system is b_{SL} Equation 2.14 which should be kept persistently excited. The easiest way to excite this input is to change the stir speed N, which is correlated with C so that oxygen demand is formed by transferring more oxygen from the sparge gas to the liquid media when N swings with a large peak to peak difference. It looks like this excitation should continue in one direction (increasing or decreasing) until it is measured by the off-gas sensor and the system dynamics (τ_h and τ_b) should be taken in consideration. This excitation is only needed at the start up when oxygen demand is very low and can not be detected by the off-gas sensor. More experiments are needed to prove this observation.

This excitation requirement is similar to the correlation needed between inputs and output

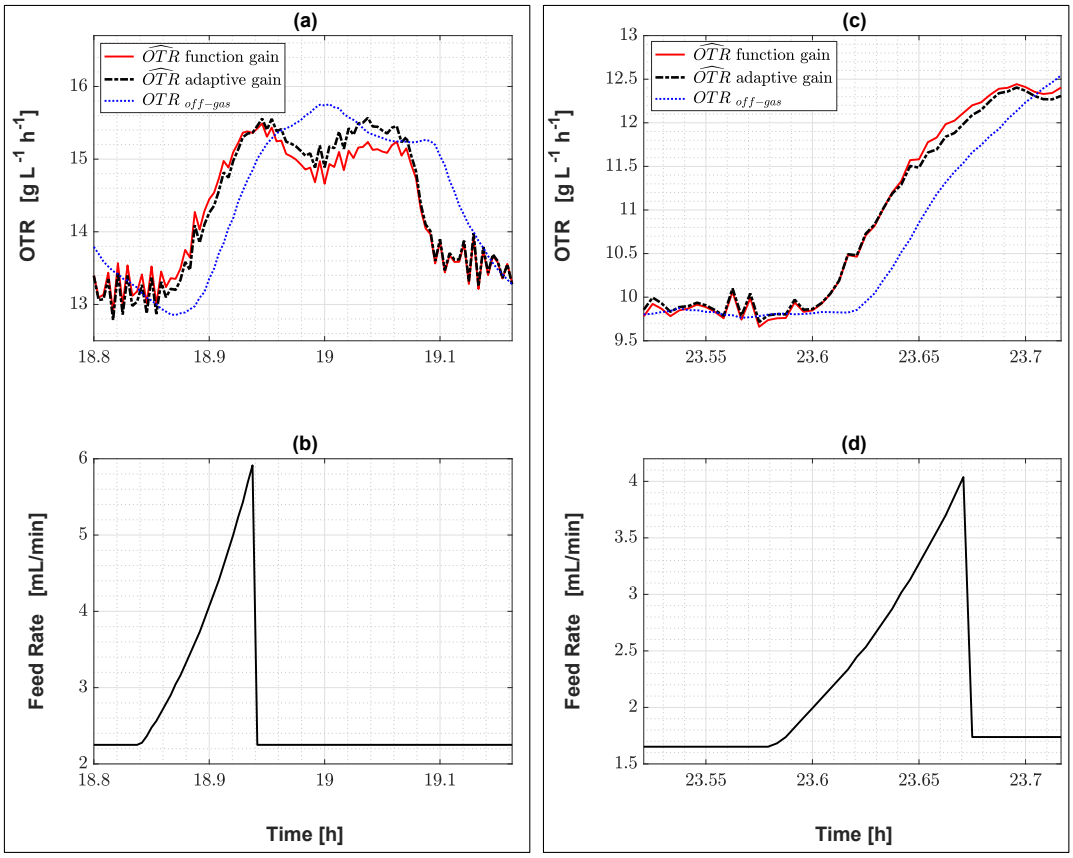

Figure 3.14: Adaptive V.S. function gain. (a) and (c) show that the estimated oxygen transfer rate red colored $\widehat{OTR}$ (using Equation 2.30), and dotted black colored $\widehat{OTR}$ (using Equation 3.2 and $F_g = 3$). Both red and dotted black colored $\widehat{OTR}$ look almost similar and are a head of that calculated using off-gas measurements $OTR_{off-gas}$. (b) and (d) show exponentially increasing probing signal using 50% [v/v] Glucose solution. Note that, (a) and (c) show the $\widehat{OTR}$ response of the probing signal shown in (b) and (d), respectively.

when regressing independent variables to predict a dependent variable. The adaptive estimator works like an on-line linear regression. So, it looks to be a requirement to excite the input in one direction until it is reflected on the output before going to the other direction.

When a PI is used to control C at a set point, any change in the oxygen demand will be, **first**, translated into a change in stir speed N, which is used to calculate $\widehat{OTR}$ as the fastest available signal, and, **second**, measured by the off-gas sensor at the exhaust. Therefore, a persistent excitation will be there in the system input b_{SL} and output b_{out}. If the PI gains are tuned very well, C will be kept close to the set point and then $\dot{C}$ will be almost equal to zero. In this case, $\widehat{OUR} =$

$\widehat{OTR}$ and $OUR_{off-gas} = OTR_{off-gas}$. However, because Zig-Zag creates a change in the oxygen demand that is not formed by the biomass, $\dot{C}$ becomes considerable and the estimated oxygen uptake rate is calculated by $\widehat{OUR} = \widehat{OTR} - \dot{C}$. But it will be difficult to calculate $OUR_{off-gas}$ because the off-gas measurement is filtered by the headspace dynamics.

3.4.3 Changing the control algorithm for less disturbed input signal

The estimator needs some time to re-converge after every change in the percentage of oxygen enrichment. So, it is suggested to use larger changes in the GasMx signal for less frequent change times. In experiment 74 as shown in Figure 3.3, for example, there was a frequent change in the GasMx signal separated by short time intervals. This increases the estimator error and limits the number of times when probing can occur.

Figure 3.15 shows a significant increase in the estimator error after an increase in the GasMx signal at cultivation time 12 [h]. The figure also shows a slight increase in the estimator error during probings and this might be due to the DO dynamics which is not considered in our design.

The PI controller of the DO level was a major source of noise. The miss tuning of the PI gains had a negative impact on the estimator error. It is suggested to check the estimator error before any probing. If the absolute value of the estimator error, for example, was less than a specific small positive number for some time to insure a good estimator convergence, then a probing can occur.

3.4.4 Value of $\hat{\alpha}$ shifts when changing GasMx

After every change in oxygen enrichment, the estimator readjusts $\hat{\alpha}$ to a lower value than that before the change in the oxygen enrichment in the sparge air as shown in Figure 3.16, which for an experiment (called Experiment 62). This might be due to scaling C^* in Equation 2.7, which is

$$C^* = K \cdot \frac{b_{in}}{b_{air}}$$

The value of K, as explained in Section 2.1, changes slowly over the course of the fermentation run due to the change in the liquid composition. However, $K = K_0$ was used as an initialization value. The exact value of K at different times, when GasMx signal changes, is unknown. The adaptive estimator, however, takes care of this issue by adjusting the value of $\hat{\alpha}$ all the

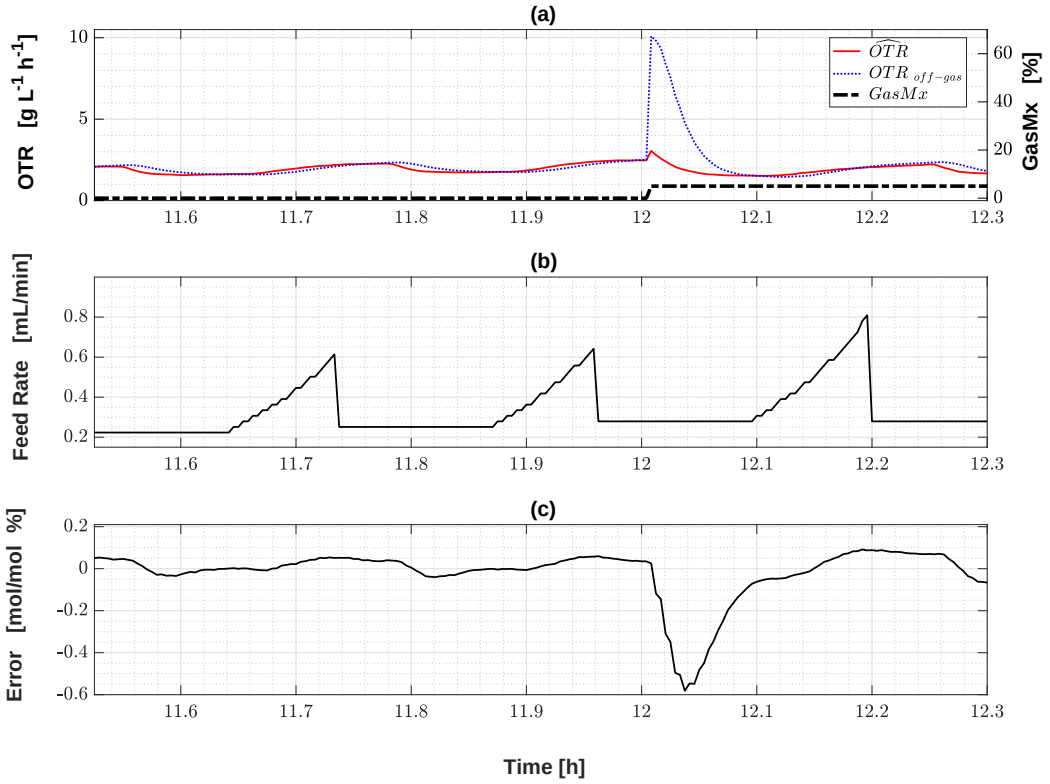

Figure 3.15: Control algorithm affects the estimator error. (a) shows the dotted black colored oxygen enrichment signal (GasMx) along with the estimated oxygen transfer rate $\widehat{OTR}$ in red color superimposed on blue colored $OTR_{off-gas}$, which is calculated using off-gas measurement of O_2. (b) shows an exponentially increasing probing signal using 50% [v/v] Glucose solution. (c) shows the error between estimated and measured value of oxygen in off-gas, calculated by Equation 2.22.

time.

The increments of GasMx signal was to increase the oxygen enrichment in the sparge air when the stir speed N approaches the maximum speed limit of the agitator. When using a PI controller to keep C at a set point, the N value is readjusted to a lower speed value. The value of $\hat{\alpha}$ should not change suddenly by the change in oxygen enrichment, however, by looking at equation

$$\widehat{OTR} = \hat{\alpha} \cdot N \cdot (K \cdot \frac{b_{in}}{b_{air}} - K_0 \cdot \frac{DO}{100}) \tag{3.4}$$

which is an expanded form of Equation 2.24, we can tell a probable reason for this change in the value of $\hat{\alpha}$. When oxygen enrichment increases, the PI controller readjusts N to a lower speed so that C, which is $K_0 \cdot \frac{DO}{100}$, is almost fixed at the set point. It looks like $\hat{\alpha}$ is readjusted due to a

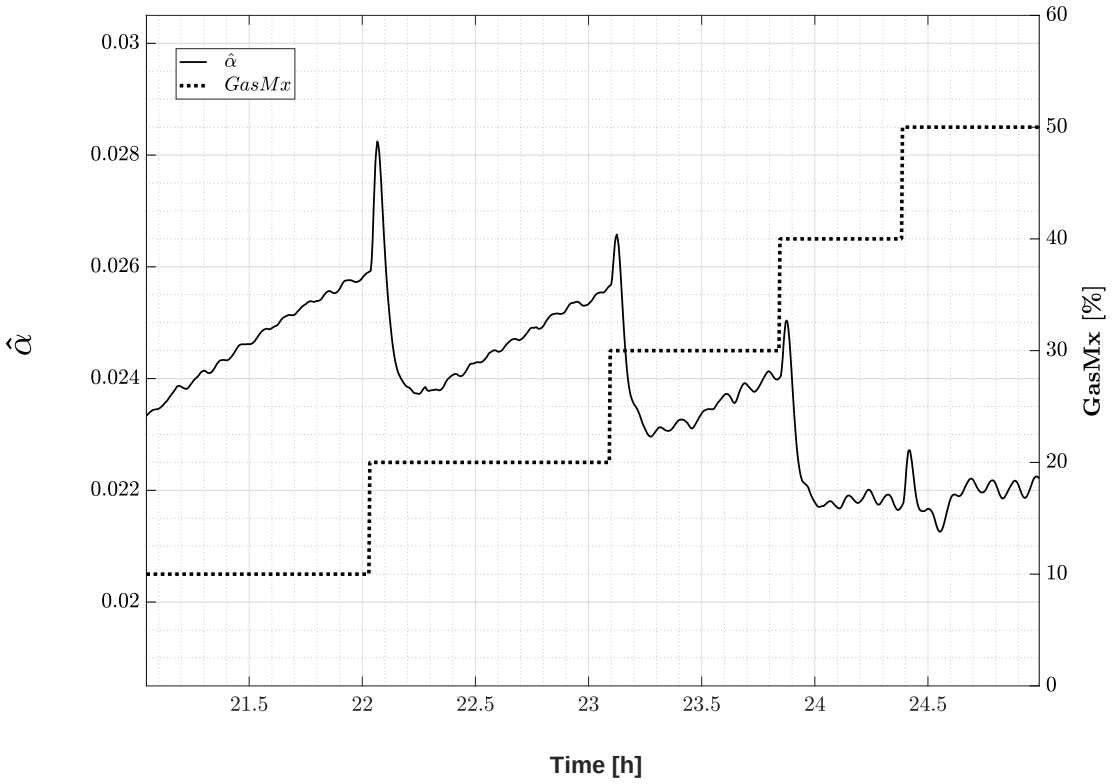

Figure 3.16: Downward shifting in $\hat{\alpha}$ value when GasMx increases.

change in the first part C^* of the driving force DF

$$DF = (K \cdot \frac{b_{in}}{b_{air}} - K_0 \cdot \frac{DO}{100}).$$

It looks like that K decreases along the course of fermentation due to change in the liquid composition and becomes unknown and less than K_0 because $K = K_0$ in our calculation. Therefore, the adaptive estimator readjusts $\hat{\alpha}$ to a lower value to compensate the wrong scaling up of C^* by the fraction $\frac{b_{in}}{b_{air}}$.

3.4.5 Difference between measurements of MFMs before and after the bioreactor

A difference was noticed between the mass flow rate measurements of input and output gases. The reason might be the specific gravity difference between the input gas and the off-gas,

which has different humidity, pressure, temperature, and gas mixture. This means a correction factor should be used to scale the measurements of the MFM of the off-gas for more accurate readings.

Chapter 4

Conclusion

In this thesis, an on-line OTR estimator, that works with oxygen enriched air, was proposed and implemented on a laboratory scale bioreactor. The method estimates the OTR or specifically k_La using measurements of oxygen concentration at the exhaust using off-gas sensor, and in the culture medium using dissolved oxygen probe. The dynamics of the bioreactor head space and the off-gas sensor were included in the design. When the estimated OTR is converged to the $OTR_{off-gas}$ computed using measurements of oxygen mole ratio by the off-gas sensor, the estimated OTR is ahead in time of the $OTR_{off-gas}$. Thus, the estimated OTR was used to detect the metabolic state of *E.coli* culture.

The dissolved oxygen DO level was controlled by a PI controller. The input air was enriched with pure oxygen to increase the OTR whenever the stir speed was close to the maximum limit. The estimator was tested in experiments with exponential feeding profile and with BOOM II controller. The estimated OTR re-converged very well after every change of the oxygen mole ratio in the input gas. Thus, the OTR was estimated for a longer time.

The proposed design is a low-cost solution for a bioreactor controller that uses solenoids to control the oxygen enrichment in the sparge air. An alternative solution could require addition of more instruments to the system. For example, another off-gas sensor could be used in the input side to measure the oxygen mole ratio of sparge gas. Another example is to use one off-gas sensor whose input is multiplexed with two gas solenoids, one solenoid for vessel exhaust and the other is for the input gas. In this case, the two solenoids work alternately so that one gas is measured at a time by the off-gas sensor. Other alternatives will require addition of mass flow controllers for more

accurate results. However, the proposed design is limited by the specifications of instruments used in the laboratory. These limits include, for example, 1 atm pressure inside the bioreactor, and 0 to 50% off-gas measurement of oxygen concentration at the bioreactor exhaust.

There was some difficulties and may be limitations of the design proposed in this thesis. The following list shows a summary of these issues:

A. The result accuracy of the proposed design is sensitive to the tuning of the mass flow rates of input air and oxygen lines.

B. PI controller of DO was a major source of noise due to gains mis-tuning.

C. The estimator is sensitive to any sudden change in the input signals. Kalman filters were used to alleviate the noise contained in the measurements of mass flow M_f by MFM, O_2 by off-gas sensor, stir speed N, and dissolved oxygen DO.

D. There was a difficulty in choosing the estimator gain, but the adaptive gain explained in Subsection 3.4.1 is recommended.

4.1 Modification Done in this Work

The differences between this work and the work developed by [Wang, 2014] include scaling the C^* by the ratio $\frac{b_{in}}{b_{air}}$ as in Equation 2.7, and using only one unknown coefficient in the linearized k_La as in Equation 2.11. The changes also include using a PI controller for the dissolved oxygen concentration level instead of using the Zig-Zag method. Another modification was by employing a decreasing over time estimator gain that is a function of the culture volume as in Equation 2.30. The most important modification was the accurate identification of the oxygen mole ratio in the sparge gas. This was done by tuning the input gases to insure equal mass flow rates, and adding a Correction factor C_f as in Equation 2.29.

4.2 Future Work

4.2.1 Difficulties in prediction of carbon dioxide concentration at liquid surface level d_{SL}

We can get a fast estimation of the partial pressure of oxygen at the liquid surface level (b_{SL}) using Equation 2.14 which is

$$b_{SL} = b_{in} - \alpha \cdot \frac{N \cdot DF}{F_r},$$

by N and DF, ignoring the dynamics of DO probe and the stir speed N, and assuming a slow changes in α which is estimated by the adaptive estimator. With an estimated value of α, Equation 2.24, which is

$$\widehat{OTR} = \hat{\alpha} \cdot N \cdot DF,$$

gives an estimation value of OTR faster than Equation 2.1

$$OTR_{off-gas} = \frac{M_f \cdot \rho_{O_2}}{V_c \cdot R \cdot T}(b_{in} - \frac{1 - b_{in} - d_{in}}{1 - b_{out} - d_{out}} \cdot b_{out}),$$

which depends on off-gas sensor measurements delayed by the total system delay.

An approximation of the CO_2 emission rate [Kamen et al., 1996] using $pC0_2$ measured by the off-gas sensor and delayed by the total system delay can be calculated by

$$CER = pC0_2 \cdot M_f \cdot \frac{1}{R \cdot T \cdot V_c} \tag{4.1}$$

The problem of estimating the carbon dioxide concentration at liquid surface level d_{SL} is, however, that we have only Equation 4.1, and we do not have a faster equation or technique to better estimate an instantaneous value of d_{SL} without time delay. In addition, the commercially available CO_2 probes that can go in the culture liquid, have no better time constant compared to that of the off-gas sensor used in our experiments.

4.2.2 Implementation under pressurized bioreactor

Our implementation was designed and tested at one atmospheric pressure. It is worth it to modify the design, if required, to enable the prediction for OTR of a cultivation running in a pressurized bioreactor with oxygen enriched input gas along. This will enable for controlling an industrial size bioreactors for further higher production of recombinant proteins.

Appendices

Appendix A Tuning Procedure for more Accuracy in b_{in} Calculation

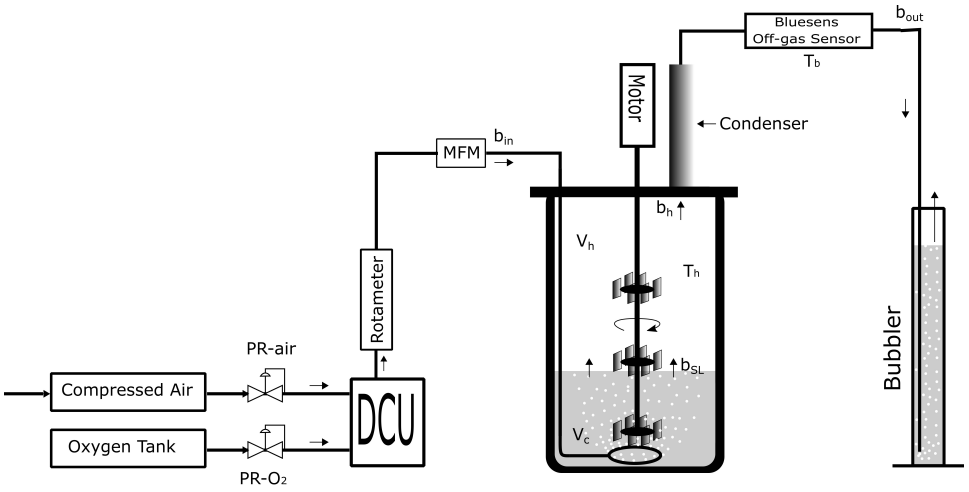

Figure 1: Bioreactor Connections.

Using the configuration shown in Figure 1, the two lines of air and oxygen can be tuned so that the predicted oxygen mole ratio in the input gas b_{in}, which is computed by Equation 2.29

$$b_{in} = \frac{(100 - GasMx) \cdot b_{air} + GasMx \cdot C_f}{100},$$

equals to the oxygen mole ratio measured by the off-gas sensor b_{out} when there is no biological consumption of oxygen. The procedure shown below was used for the tuning, however, this is not necessarily to be the best procedure. The procedure was tested for GasMx values up to 40% which gives around 51% of oxygen mole ratio in the input gas. This was limited by our particular off-gas sensor, where the maximum safe range of oxygen concentration measurement is 50%. The procedure is: -

A. Hardware limits must always be considered during this procedure, i.e., maximum measurements of off-gas sensor, and MFM, and the maximum pressure of the bioreactor vessel.

B. Start by flowing only air and the pure oxygen line is closed, i.e., $GasMx = 0$.

C. Use the rotameter to measure the desired mass flow rate of air M_{f-air}, which can be adjusted with air pressure regulator PR-air, rotameter and DCU aeration knobs. After this step, these

knobs should not be changed.

D. Open oxygen line.

E. Using only the oxygen pressure regulator PR-O_2 knob, adjust the oxygen mass flow rate M_{f-O_2} so that the rotameter measurement reads $M_{f-O_2} = M_{f-air}$.

F. If there was a difficulty in achieving $M_{f-O_2} = M_{f-air}$, then consider changing the mass flow rate of air by repeating this procedure from step B.

Appendix B Estimator Algorithm and Simulink Blocks

The algorithm was implemented on Simulink. Figure 2 shows the blocks used to implement the adaptive estimator explained in Chapter 2. The following list explains the blocks according to the alphabet letter of each block as shown in Figure 2.

A. Inputs of the adaptive estimator are marked in green color. They are off-gas sensor measurement of oxygen [O2], stir speed [N], dissolved oxygen probe measurement [DO], mass flow rate [MF] measured by MFM, estimated liquid volume [Vc_hat], oxygen enrichment signal [GasMx].

B. Kalman filters are used to alleviate the noise contained in some of the input signals. [O2], [N] and [DO] are slightly filtered, but [MF] is heavily filtered because it is not expected to change during the cultivation time.

C. Pre-calculations needed for the estimator as shown in the following Matlab code.

```
function [f1,f2,Fr,Tau_h,DF,b_i,Gain] = ...
    preCalc(GasMx,DO_KF,Hery_law,FermSim_w2,N_KF,FermSim_Vt,Vc_hat,MF_KF)
% MM. Modifications 09 April 2017 for kLa estimator

%% ############# Mass Flow Rate #################
% To solve the problem of division by zero,
% we use 4 [L/min] as the minimum mass flow rate
if (MF_KF ≤ 4)
    Mf_LperH = 4*60;    % Mf_LperH is the mass flow rate [L/h]
else
    Mf_LperH = MF_KF*60;
end

%% ############# Time Constants #################
Tau_h = (FermSim_Vt-Vc_hat)/(Mf_LperH/3600);    % FermSim_Vt is the veesel ...
    total volume, and Vc_hat is the estimated liquid volume.
Tau_h_inv = 1/Tau_h;    % Tau_h is head space time constant
Tau_b_inv = FermSim_w2; % Tau_b is Off-gas sensor time constant = 55 sec ...
    (FermSim.w2 = 1/55 seconds)

%% ############# Driving Force DF #################
```

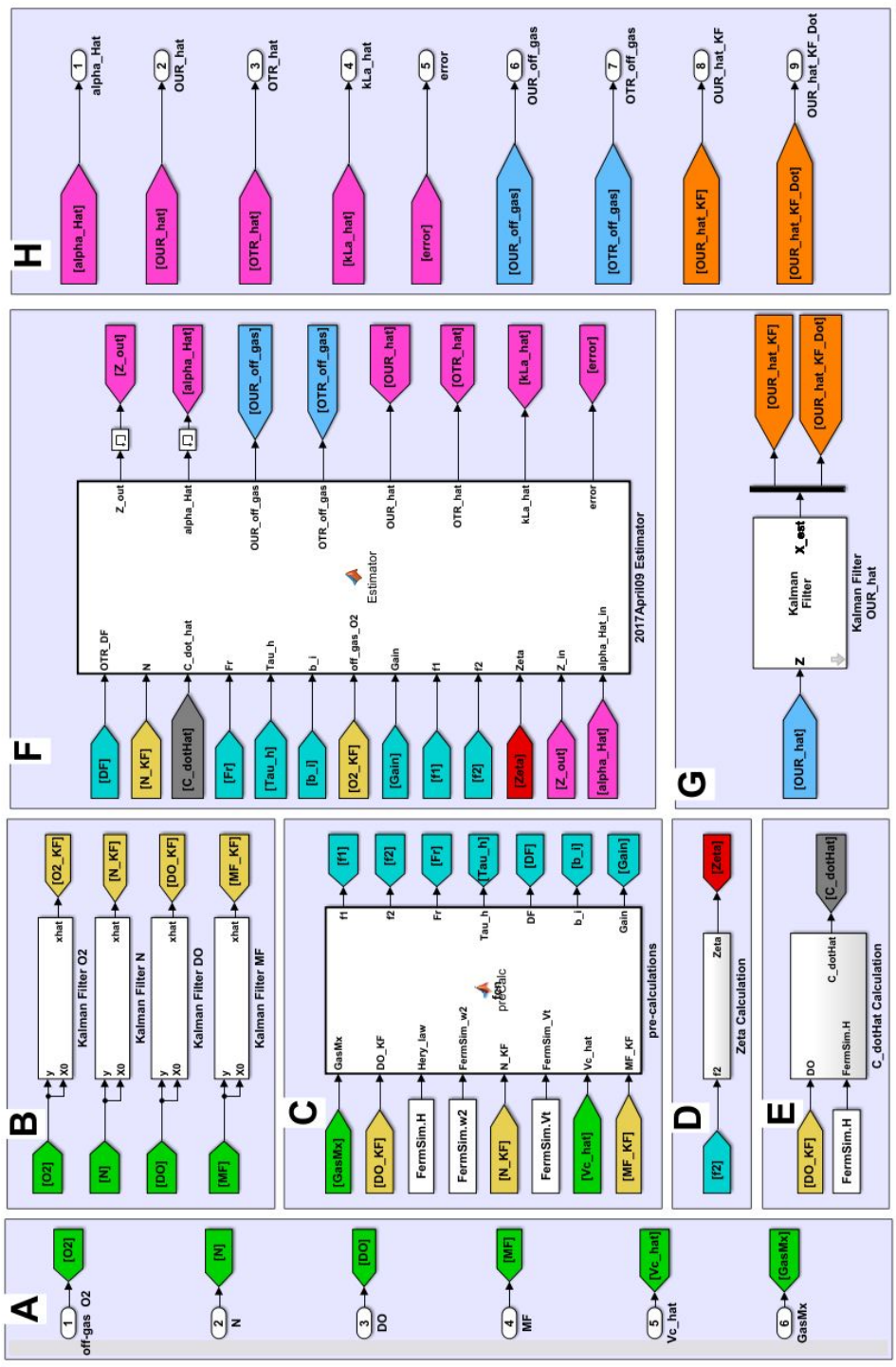

Figure 2: Simulink model of the adaptive estimator.

```
C = DO_KF/Hery_law;    % Equation 2.8, where Hery_law = 100/K
C_f = 0.9706;   % Equation 2.27
b_air = 0.209627;   %
b_i = (((100-GasMx)*b_air+GasMx*C_f)/100);  % Equation 2.29
C_star = (100/Hery_law)*(b_i/b_air);    % Equation 2.7
DF = C_star - C;    % Equation 2.9

%% ############# Calculate Scaling Fraction #################
Fr = (Mf_LperH*1.0133)/(Vc_hat*8.314e-2*(273.15+37));   % Equation 2.4

%% ############# Calculate f matrix #################
f1 = Tau_b_inv*Tau_h_inv;   % Equation 2.19
f2 = -1*Tau_b_inv*Tau_h_inv*DF*N_KF/Fr;   % Equation 2.19

%% ############# Calculate Gain Function #################
Gain = 300/Vc_hat^14+.01;   % Equation 2.3
```

D. Filter bank $G(s)$ to generate Zeta ζ implemented in discretized transfer function is shown in Figure 3. To add a continuous to digital transfer function block in Simulink, use the command "discretizing" in Matlab command window. Select "tustin Discretized Transfer Fcn" and change it to "zoh" and fill in both denominator and nominator with polynomials in S-plane.

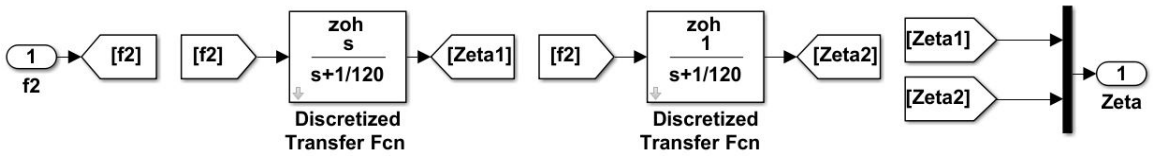

Figure 3: Simulink discrete transfer function for ζ.

E. Discrete derivative to compute $\dot{C}$ as shown in Figure 4.

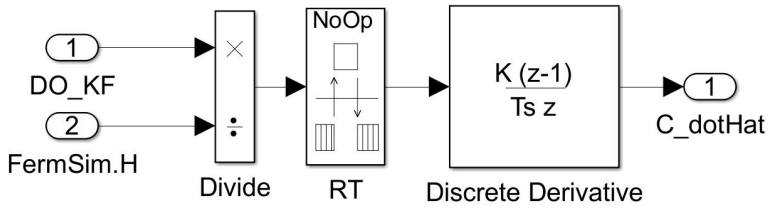

Figure 4: Simulink discrete derivative function for $\dot{C}$ computation. FermSim.H is $\frac{100}{K_0}$, where $K_0 = 2.1 \times 10^{-4}$ $[\text{mol} \cdot \text{L}^{-1}]$

F. Calculations of the adaptive estimator are shown in the following Matlab code.

```
function ...
    [Z_out,alpha_Hat,OUR_off_gas,OTR_off_gas,OUR_hat,OTR_hat,kLa_hat,error] = ...
    Estimator(OTR_DF,N,C_dot_hat,Fr,Tau_h, ...
    b_i,off_gas_O2,Gain,f1,f2,Zita,Z_in,alpha_Hat_in,FermSim)
% MM. Modifications 09 April 2017 for kLa estimator

T_sample = 15;  % Sampling time 15 seonds

%% ############# Time Constants #################
Tau_b_inv = FermSim.w2; % Tau_b is Off-gas sensor time constant = 55 sec ...
    (FermSim.w2 = 1/55 seconds)
Tau_h_inv = 1/Tau_h;    % Tau_h is head space time constant
d2=1/120;   % d2 value used in the filter bank G(s) and A2 matrix
%% ############# Time Constants #################
bo_hat = Z_in(1);   % The estimated oxygen mole ratio at the exhaust
b_out = off_gas_O2/100; % oxygen mole ratio measured by the off-gas sensor at ...
    the exhaust
error = bo_hat - b_out; % Equation 2.22 the estimator error

%% ############# The Gain Matrix #################
Lambda = [Gain 0; 0 Gain];  % Equation 2.21 the Gain matrix Lambda
% % % If adaptive gain is required, then Lambda22 is added to the output
% % % signals and fed-back to the estimator block via a memory. An input signal
% % % Lambda22_in is added, then the following lines are used instead of
% % % the line 16- Lambda = [Gain 0; 0 Gain];   % Equation 2.21
% Lambda_in = [0 0;0 Lambda22_in];
% Lambda_dot = -Lambda_in*Zita*Zita'*Lambda_in; % Equation 3.2
% Lambda = Lambda_in + Lambda_dot*T_sample; % Discrete intergation of ...
    Equation 3.2
% Lambda22 = Lambda(2,2);

%% ############# Head Space Linear Model #################
A = [-(Tau_h_inv+Tau_b_inv) 1; -(Tau_h_inv*Tau_b_inv) 0];   % Equation 2.19
B = [0 0;b_i alpha_Hat_in];   % Equation 2.19
f = [f1;f2];   % Equation 2.19

```

```
%% ############# The Adaptive Estimator #################
% we need one auxiliary variable in the observer bacause we have only one
% uknown coefficient (alpha)
A2 = [0 -d2; 0 1];  % A2 matrix used in M matrix
M = [0;-error*Zita'*Lambda*A2*Zita];    % M matrix used in Equation 2.20
Z_dot = A*Z_in + B*f + M;   % Equation 2.20
Z_out = Z_in + Z_dot*T_sample;  % Discrete intergation of Equation 2.20

%% ############# The Adaptive Law #################
S = [0 1];  % used to convert Lambda*Zita in Equation 2.23 into a scaler
alpha_Hat_dot = - error*S*Lambda*Zita;  % Equation 2.23
% % % If an adaptive gain was implemented, then
% alpha_Hat_dot = - error*F_g*S*Lambda*Zita;  % Equation 3.3, where F_g is ...
    any positive number selected by trial and error
alpha_Hat = alpha_Hat_in + alpha_Hat_dot*T_sample;  % Discrete intergation of ...
    Equation 2.23

%% ############# OUR & OTR Calculations #################
kLa_hat = alpha_Hat*N;  % Equation 2.11
OTR_hat = kLa_hat*OTR_DF;  % Equation 2.24
OUR_hat = OTR_hat - (C_dot_hat/240);  % Equation 2.25, where the division by ...
    240 is to get change per hour
OTR_off_gas = Fr*(b_i-b_out);   % Equation 2.3
OUR_off_gas = OTR_off_gas;  % this is valid only when C_dotHat is almost zero

%% ############# Convert [mol/(L*h)] into [g/(L*h)] #################
OTR_hat = OTR_hat*32;   % *32 to get g/(L*h)
OUR_hat = OUR_hat*32;   % *32 to get g/(L*h)
OTR_off_gas = OTR_off_gas*32;   % *32 to get g/(L*h)
OUR_off_gas = OUR_off_gas*32;   % *32 to get g/(L*h)
```

G. Kalman filter for slight final filtration of $\widehat{OUR}$ and to generate $\dot{\widehat{OUR}}$ simultaneously during the filtration process.

H. Output signals $\hat{\alpha}$ [alpha_hat], $\widehat{OUR}$ [OUR_hat], $\widehat{OTR}$ [OTR_hat], k_La [kLa_hat], $\mathbf{e}$ [error], $OUR_{off-gas}$ [OUR_off_gas], $OTR_{off-gas}$ [OTR_off_gas], Kalman filtered $\widehat{OUR}$ [OUR_hat_KF], and first derivative of $\widehat{OUR}$ computed by the Kalman filter block for faster calculation [OUR_hat_KF_Dot].

Appendix C List of Experiments Used for this Thesis

Table 1 summarizes the settings and conditioning of experiments used in this thesis.

	Experiment				
	5	**58**	**60**	**62**	**74**
***DO* controller**	Steps [1]	N/A [4]	PI [3]	PI [3]	PI [3]
Inoculation	Yes	No	Yes	Yes	Yes
Induction	No	N/A [4]	No	No	Yes
Feeding profile	EFP [5]	N/A [4]	EFP [5]	EFP [5]	BOOM II [6]
Time [h]	20.76	2.38	22.91	27.43	23.8

Table 1: Experiments summary.

[1] Stir speed was changed in steps so that *DO* was kept bounded between 40% to 70%.

[2] Stir speed was continuously ramping up and down so that *DO* was kept bounded between 40% to 70%.

[3] *DO* was kept at a set point and controlled via a PI controller embedded in the DCU.

[4] Not applicable because there were no cells in the liquid and there was no biological consumption of oxygen.

[5] Exponential feeding profile.

[6] Feed rate was controlled via BOOM II algorithm so that *E.coli* grows at nearly optimal rate.

Bibliography

[Åkesson and Hagander, 1999] Åkesson, M. and Hagander, P. (1999). A gain-scheduling approach for control of dissolved oxygen in stirred bioreactors. In *Preprints 14th World Congress of IFAC*, pages 505–510.

[Badino et al., 2000] Badino, A. C., Facciotti, M., and Schmidell, W. (2000). Improving kla determination in fungal fermentation, taking into account electrode response time. *Journal of Chemical Technology and Biotechnology*, 75(6):469–474.

[Bandyopadhyay et al., 1967] Bandyopadhyay, B., Humphrey, A., and Taguchi, H. (1967). Dynamic measurement of the volumetric oxygen transfer coefficient in fermentation systems. *Biotechnology and bioengineering*, 9(4):533–544.

[Bastin and Dochain, 1990] Bastin, G. and Dochain, D. (1990). *On-line Estimation and Adaptive Control of Bioreactors.* Elsevier Science.

[Belo and Mota, 1998] Belo, I. and Mota, M. (1998). Batch and fed-batch cultures of e. coli tb1 at different oxygen transfer rates. *Bioprocess and Biosystems Engineering*, 18(6):451–455.

[Benson and Krause, 1980] Benson, B. B. and Krause, D. (1980). The concentration and isotopic fractionation of gases dissolved in freshwater in equilibrium with the atmosphere. 1. oxygen. *Limnology and Oceanography*, 25(4):662–671.

[BlueSens, nd] BlueSens (nd). *Manual BlueVis.* BlueSens gas sensor GmbH Snirgelskamp 25 D-45699 Herten, Germany Phone +49 2366 4995 500 Fax +49 2366 4995 599 www.bluesens.de.

[Carbajal and Tecante, 2004] Carbajal, R. and Tecante, A. (2004). On the applicability of the dynamic pressure step method for k l a determination in stirred newtonian and non-newtonian fluids, culture media and fermentation broths. *Biochemical engineering journal*, 18(3):185–192.

[Castan et al., 2002] Castan, A., Näsman, A., and Enfors, S.-O. (2002). Oxygen enriched air supply in escherichia coli processes: production of biomass and recombinant human growth hormone. *Enzyme and microbial technology*, 30(7):847–854.

[Ertunc et al., 2009] Ertunc, S., Akay, B., Boyacioglu, H., and Hapoglu, H. (2009). Self-tuning control of dissolved oxygen concentration in a batch bioreactor. *Food and Bioproducts Processing*, 87(1):46–55.

[Franklin et al., 2011] Franklin, G. F., Powell, J. D., and Emami-Naeini, A. (2011). *Feedback control of dynamic systems.* Pearson Higher.

[Garcia-Ochoa and Gomez, 2009] Garcia-Ochoa, F. and Gomez, E. (2009). Bioreactor scale-up and oxygen transfer rate in microbial processes: an overview. *Biotechnology advances*, 27(2):153–176.

[Gharakozlou Lashkari, 2017] Gharakozlou Lashkari, S. (2017). Controlling recombinant escherichia coli cultures to the boundary of oxidative and overflow metabolism (boom) for robust efficient growth. Master's thesis, Clemson University.

[Jensen and Carlsen, 1990] Jensen, E. B. and Carlsen, S. (1990). Production of recombinant human growth hormone in escherichia coli: expression of different precursors and physiological effects of glucose, acetate, and salts. *Biotechnology and bioengineering*, 36(1):1–11.

[Ju et al., 1991] Ju, L. K., Lee, J. F., and Armiger, W. B. (1991). Enhancing oxygen transfer in bioreactors by perfluorocarbon emulsions. *Biotechnology Progress*, 7(4):323–329.

[Kamen et al., 1996] Kamen, A. A., Bédard, C., Tom, R., Perret, S., and Jardin, B. (1996). On-line monitoring of respiration in recombinant-baculovirus infected and uninfected insect cell bioreactor cultures. *Biotechnology and bioengineering*, 50(1):36–48.

[Kim and Chang, 1989] Kim, D.-J. and Chang, H.-N. (1989). Dynamic measurement of kla with oxygen-enriched air during fermentation. *Journal of chemical technology and biotechnology*, 45(1):39–44.

[Knoll et al., 2007] Knoll, A., Bartsch, S., Husemann, B., Engel, P., Schroer, K., Ribeiro, B., Stöckmann, C., Seletzky, J., and Büchs, J. (2007). High cell density cultivation of recombinant yeasts and bacteria under non-pressurized and pressurized conditions in stirred tank bioreactors. *Journal of biotechnology*, 132(2):167–179.

[Kudva and Narendra, 1973] Kudva, P. and Narendra, K. S. (1973). Synthesis of an adaptive observer using lyapunov's direct method. *International Journal of Control*, 18(6):1201–1210.

[Kumar et al., 2008] Kumar, S. G., Jain, R., Anantharaman, N., Dharmalingam, V., and Begum, K. (2008). Genetic algorithm based pid controller tuning for a model bioreactor. *indian chemical engineer*, 50(3):214–226.

[Lara et al., 2011] Lara, A. R., Knabben, I., Regestein, L., Sassi, J., Caspeta, L., Ramírez, O. T., and Büchs, J. (2011). Comparison of oxygen enriched air vs. pressure cultivations to increase oxygen transfer and to scale-up plasmid dna production fermentations. *Engineering in Life Sciences*, 11(4):382–386.

[Luli and Strohl, 1990] Luli, G. W. and Strohl, W. R. (1990). Comparison of growth, acetate production, and acetate inhibition of escherichia coli strains in batch and fed-batch fermentations. *Applied and environmental microbiology*, 56(4):1004–1011.

[Narendra and Annaswamy, 2012] Narendra, K. S. and Annaswamy, A. M. (2012). *Stable adaptive systems*. Courier Dover Publications.

[Ortiz-Ochoa et al., 2005] Ortiz-Ochoa, K., Doig, S. D., Ward, J. M., and Baganz, F. (2005). A novel method for the measurement of oxygen mass transfer rates in small-scale vessels. *Biochemical Engineering Journal*, 25(1):63–68.

[Patel and Thibault, 2009] Patel, N. and Thibault, J. (2009). Enhanced in situ dynamic method for measuring k_La in fermentation media. *Biochemical Engineering Journal*, 47(1):48–54.

[Pedersen et al., 1994] Pedersen, A. G., Andersen, H., Nielsen, J., and Villadsen, J. (1994). A novel technique based on 85kr for quantification of gasliquid mass transfer in bioreactors. *Chemical engineering science*, 49(6):803–810.

[Pepper, 2015] Pepper, M. E. (2015). *Designing a Minimal-Knowledge Controller to Achieve Fast, Stable Growth for Recombinant Escherichia coli Cultures*. PhD thesis, Clemson University.

[Pramod and Chidambaram, 2000] Pramod, S. and Chidambaram, M. (2000). Closed loop identification of transfer function model for unstable bioreactors for tuning pid controllers. *Bioprocess and Biosystems Engineering*, 22(2):185–188.

[Redmon et al., 1983] Redmon, D., Boyle, W. C., and Ewing, L. (1983). Oxygen transfer efficiency measurements in mixed liquor using off-gas techniques. *Journal (Water Pollution Control Federation)*, pages 1338–1347.

[Sanchez-Garcia et al., 2016] Sanchez-Garcia, L., Martín, L., Mangues, R., Ferrer-Miralles, N., Vázquez, E., and Villaverde, A. (2016). Recombinant pharmaceuticals from microbial cells: a 2015 update. *Microbial cell factories*, 15(1):33.

[Stewart A. Rounds and Ritz, 2013] Stewart A. Rounds, F. D. W. and Ritz, G. F., editors (2013). *U.S. Geological Survey Techniques of Water-Resources Investigations, Book 9, chap. A6., sec. 6.2.* accessed [date viewed], from `https://water.usgs.gov/owq/FieldManual/Chapter6/6.2_ver3.pdf`. (March 21, 2017.).

[Van Suijdam et al., 1978] Van Suijdam, J., Kossen, N., and Joha, A. (1978). Model for oxygen transfer in a shake flask. *Biotechnology and Bioengineering*, 20(11):1695–1709.

[Van't Riet, 1979] Van't Riet, K. (1979). Review of measuring methods and results in nonviscous gas-liquid mass transfer in stirred vessels. *Industrial & Engineering Chemistry Process Design and Development*, 18(3):357–364.

[Vashitz et al., 1989] Vashitz, O., Sheintuch, M., and Ulitzur, S. (1989). Mass transfer studies using cloned-luminous strain of xanthomonas campestris. *Biotechnology and bioengineering*, 34(5):671–680.

[Wang, 2014] Wang, L. (2014). Design and implementation of a real-time adaptive oxygen transfer rate estimator. Master's thesis, Clemson University.

[Zumdahl, 2014] Zumdahl, Steven S., Z. S. A. B. P. C. (2014). *Chemistry*. Brooks/Cole Cengage Learning, Belmont. ID: 904770482.